- Dissertation -

AUS DEM LEHRSTUHL
FÜR DERMATOLOGIE UND VENEROLOGIE
PROF. DR. MARK BERNEBURG
DER FAKULTÄT FÜR MEDIZIN
DER UNIVERSITÄT REGENSBURG

EXPRESSIONSPROFILE PROTONEN-SENSITIVER G-PROTEIN-GEKOPPELTER REZEPTOREN IN HÄUFIG VORKOMMENDEN HAUTTUMOREN

Inaugural-Dissertation
zur Erlangung des Doktorgrades
der Zahnmedizin

der
Fakultät für Medizin
der Universität Regensburg

vorgelegt von
Wybke Klatt

2020

- Dissertation -

AUS DEM LEHRSTUHL
FÜR DERMATOLOGIE UND VENEROLOGIE
PROF. DR. MARK BERNEBURG
DER FAKULTÄT FÜR MEDIZIN
DER UNIVERSITÄT REGENSBURG

EXPRESSION PROFILES OF PROTON-SENSING G-PROTEIN-COUPLED RECEPTORS IN COMMON SKIN TUMORS

Inaugural-Dissertation
zur Erlangung des Doktorgrades
der Zahnmedizin

der
Fakultät für Medizin
der Universität Regensburg

vorgelegt von
Wybke Klatt

2020

Dekan:	Prof. Dr. Dirk Hellwig
1. Berichterstatter:	Prof. Dr. Stephan Schreml
2. Berichterstatter:	Priv.-Doz. Dr. Frank Haubner
Tag der mündlichen Prüfung:	20.01.2021

Inhaltsverzeichnis

1. Einleitung

In dieser Arbeit wurde mittels immunhistochemischer und -fluoreszenter histologischer Verfahren das Expressionsprofil membranständiger Protonen-sensitiver G-Protein-gekoppelter Rezeptoren (pH-GPCRs) in häufig vorkommenden Hauttumoren untersucht.

Im vergangenen Jahrzehnt zeigte sich eine zunehmende Inzidenz von Hauttumoren.[1,2] Die vier hier untersuchten Hauttumoren sind spinozelluläre Karzinome (SCC), Basalzellkarzinom (BCC), Nävuszellnävie (NCN) und Melanome (MM). SCC sind von der Epidermis ausgehende, squamös differenzierte Tumoren, die ab einer Tumordicke von 2 mm häufiger metastasieren.[3] Die semimalignen BCC sind durch ein langsames und destruierendes Wachstumsverhalten charakterisiert und mit Abstand die häufigsten Hauttumoren. Metastasierungen treten nur extrem selten auf.[4] NCN sind gutartige, angeborene oder erworbene Vermehrungen von Melanozyten in Epidermis und/oder Dermis mit Nestbildung.[5] MM entwickeln sich in einem Teil der Fälle aus NCN, großteils allerdings de novo.[6] Obwohl nur 2 % aller Hauttumoren MM sind, ist es einer der tödlichsten Hauttumore aufgrund der frühzeitigen systemischen Metastasierung.[7,8]

Protonen-sensitive G-Protein-gekoppelten Rezeptoren sind eine der vielfältigsten Familien membranständiger Rezeptoren an Zelloberflächen und kommen bei verschiedenen Eukaryoten, einschließlich Tieren, Pflanzen, Pilzen und dem Menschen vor.[9,10]

Die pH-GPCRs GPR4 (GPR19), TDAG8 (GPR65, T-cell death associated gene 8), OGR1 (GPR68, ovarian cancer GPCR1) und G2A (GPR132, G2 accumulation protein) werden durch Protonen aus dem Extrazellulärraum aktiviert und nehmen über Histidinreste auf ihrer Oberfläche den extrazellulären pH-Wert (pH_e) wahr.[11] Die Zentralfunktion der Protonensensoren im gesunden Organismus scheint die Aufrechterhaltung der zellulären Homöostase zu sein. Jedoch glaubt man, dass in Tumoren gewisse Funktionen der pH-GPCRs helfen, den Zellen einen Wachstumsvorteil zu verschaffen, während andere das Wachstum hemmen.[12,13]

Die unzureichende Vaskularisierung eines Tumors bei mangelhafter Oxygenierung führt zur Hypoxie und die Tumorzellen müssen ATP vorwiegend über die anaerobe Glykolyse bereitstellen. Dies wiederum führt zur anschließenden Ausscheidung von saurem Laktat in den Extrazellulärraum.[14,15] Durch das Zusammenspiel mehrerer Proteine können Tumorzellen diese

anfallenden sauren Substanzen eliminieren. Zu den pH-regulatorischen Transportern zählen der Monocarboxylat-Transporter (MCT1+4), der Na^+/H^+-Austauscher 1 (NHE1), eine Vakuolen-ATPase (V-ATPase) sowie die Carboanhydrasen II, IX und XII.[14,16] Diese Elimination saurer Metaboliten führt dazu, dass sich der extra – (pH_e) und intrazelluläre (pH_i) pH-Wert in Tumoren gegenüber dem im gesunden Gewebe unterscheidet.

Während normal differenzierte Zellen einen pH_i in einem begrenzten Bereich von 6,9 – 7,2 im Vergleich zu einem pH_e von 7,2 – 7,4 aufweisen, verfügen Tumorzellen über ein saureres extrazelluläres Milieu (pH_e 6,2 – 7,0) und eine signifikante intrazelluläre Alkalisierung (pH_i 7,2 – 7,7).[17] Diese Regulationsstörung wird als umgekehrter oder "inside-out" pH-Gradient (pHe < pHi) bezeichnet.[18] Die Anpassung der Tumorzellen an die extrazelluläre Übersäuerung fördert teils die Weiterentwicklung des Tumors durch Beeinflussung des Zellumsatzes und Begünstigung der Metastasierung.[13,14,16,18,19]

Die pH-GPCRs sind beteiligt an der Tumorzellproliferation, Adhäsion, Migration, Metastasierung und der Modulation des Immunsystems.[11,13,21-23,25] Dennoch ist es weiterhin ungeklärt, wie die individuelle pH-GPCR Expression mit einer bestimmten Tumorzellfunktion in Verbindung steht.[11,13,21-23,25]

Die pH-GPCRs GPR4, TDAG8, OGR1 und G2A scheinen in der Haut exprimiert zu werden. Allerdings existieren nur wenige Daten zur Proteinexpression in Hauttumoren beziehungsweise verschiedenen Hautzelltypen.[13] Unser Labor lieferte bereits erste Nachweise zur Expression auf Proteinebene von pH-GPCRs in ausgewählten seltenen Hauttumoren: Merkelzellkarzinom (MCC), Dermatofibrosarcoma protuberans (DFSP), atypisches Fibroxanthom (AFX) und pleomorphes dermales Sarkom (PDS).[20]

Das Ziel dieser Studie war es nun mit Immunhistochemie und –fluoreszenz, das Vorhandensein der jeweiligen pH-GPCRs in Gewebeproben der vier obengenannten Hauttumorentitäten zu analysieren: SCC, BCC, NCN und BCC. Die Ermittlung der charakterischen Expressionsmuster der vier verschiedenen pH-GPCRs könnte zu einer besseren histologischen Differenzierung beitragen (e.g. NCN und MM) und neuen Zielstrukturen für Antikörpertherapien ermitteln.

2. Material und Methoden

2.1) Gewebeproben

Insgesamt wurden für unsere Testungen Gewebeproben der o.g. Tumoren (IHC/IF: n = 5, Ausnahme: BCC n = 6; TMA: n = 24-27) des dermatopathologischen Labors der Klinik und Poliklinik für Dermatologie, Universitätsklinikum Regensburg verwendet. Eingeschlossen in die Studie wurden lediglich Gewebeschnitte, die älter als 10 Jahre waren.

Die folgenden Gewebetypen dienten als Positivkontrollen: primär menschliches Mandelgewebe und Lungengewebe für G2A und TDAG8, die endosomale Membran des Hodens und der Lunge für OGR1 und der Pankreas sowie die endosomale Membran der Lunge für GPR4. Als Negativkontrolle für GPR4 fungierte Lebergewebe, für GPR65 Herzmuskelgewebe, für GPR68 Pankreas und für GPR132 Ovarialgewebe. Sowohl die Negativ- als auch die Positivkontrollen werden in der nachfolgend angehängten Publikation, unter dem Abschnitt der ergänzenden Informationen (Abb. S19), bildlich dargestellt.

2.2) Immunhistochemie (IHC)

Hämatoxylin-Eosin (HE)-gefärbte, in Paraffin eingebettete Gewebeproben sowie Positiv- und Negativkontrollen wurden in 2 µm dünne Stücke geschnitten und auf Objektträger gebracht. Die Proben wurden für 30 Minuten bei 72 °C inkubiert, bevor sie mit einer Alkohollösung absteigender Konzentration wie folgt rehydratisiert worden sind: 2 x Xylol für 5 Minuten, 2 x 100 % Ethanol für 5 Minuten, 2 x 96 % Ethanol für 5 Minuten, 2 x 70 % Ethanol für 5 Minuten. Die endogene Peroxidase wurde dann mit 3 % H_2O_2 (Fisher Scientific GmbH, Schwerte, Deutschland) für 10 Minuten neutralisiert. Danach wurden die Proben in destilliertem Wasser gewaschen und anschließend für 20 Minuten in Citratpuffer (Zytomed Systems GmbH, Berlin, Deutschland) gekocht. Nachdem die Schnitte auf Eis gekühlt worden sind, folgte die Inkubation in PBS (Sigma-Alrich, St. Louis, Vereinigte Staaten von Amerika). Anschließend wurden die Schnitte in Shandon-Coverplates (Fisher Scientific GmbH, Schwerte, Deutschland) eingespannt und ein weiteres Mal mit PBS gewaschen. Die Proben wurden in einer Blocking-Lösung (ZytoChem Plus HRP Kit/Rabbit, Zytomed Systems GmbH, Berlin, Deutschland) für 10 Minuten bei Raumtemperatur inkubiert, um die unspezifische Bindung von Antikörpern zu minimieren.

Im Folgenden wurden die Gewebeproben mit primären polyklonalen Antikörpern “rabbit anti-human“ für GPR4, GPR65, GPR68 und GPR132 bei 4 °C über Nacht behandelt. Am nächsten

Tag wurden die Schnitte in PBS (3 x 5 Minuten) gespült und dann mit dem sekundären biotinylierten Antikörper (ZytoChem Plus HRP Kit/Rabbit, Zytomed Systems GmbH, Berlin, Deutschland) für 30 Minuten bei Raumtemperatur inkubiert. Nach dreimaligem Waschen mit PBS, wurden die Proben mit Streptavidin-HRP-Konjugat für 20 Minuten bei Raumtemperatur inkubiert, gefolgt von einem weiteren Waschschritt mit PBS. Schließlich wurde die Chromogenlösung AEC plus (Dako, Glostrup, Dänemark) hinzugefügt. Die Reaktion wurde durch mehrmaliges Waschen mit destilliertem Wasser gestoppt, sobald die Positivkontrollen eine deutliche Färbung aufwiesen. Mayer's Haemalm (Merck KGaA, Darmstadt, Deutschland) wurde zum Gegenfärben der Gewebe benutzt. Die Proben wurden in Aquatex-Eindeckmedien eingebettet.

2.3) Gewebe-Mikroarray (TMA)

Die immunhistochemische Gewebe-Mikroarray Technologie (TMA) ermöglicht die gleichzeitige IHC-Färbung mehrerer Gewebeproben. Repräsentatives Tumormaterial aus 24 – 27 Gewebeproben pro Tumortyp wurde in einem einzigen Paraffinblock eingebettet. Proben auf den TMA-Gewebeträger wurden gemäß dem oben genannten Protokoll der IHC-Färbung unterzogen.

2.4) Immunfluoreszenz (IF)

Die Proben wurden in einem Wärmeschrank für 20 Minuten bei 70 °C inkubiert und danach mit einer absteigenden Alkoholkonzentration wie folgt behandelt: 2 x Xylol für 5 Minuten, 2 x 100 % Ethanol für 5 Minuten, 2 x 96 % Ethanol für 5 Minuten, 2 x 70 % Ethanol für 5 Minuten. Die Objektträger wurden mit PBS gewaschen und anschließend in Citrat-Tris-EDTA-Pufferlösung (Zytomed Systems GmbH, Berlin, Deutschland) überführt. Die Schnitte wurden für 25 Minuten auf Eis gestellt und dann in PBS für 10 Minuten eingetaucht. Zur Vermeidung von Autofluoreszenzen wurden die Proben für 15 Minuten in Tris-Glycin-Puffer (Trishydroxymethylaminomethan: Merck KGaA, Darmstadt, Deutschland; Glycine: Merck KGaA, Darmstadt, Deutschland) inkubiert. Nach drei Spülungen mit PBS wurden die Proben in 5% BSA (Sigma-Aldrich, St. Louis, Vereinigte Staaten von Amerika) in TBST (Tween-20: Carl Roth GmbH & Co., Karlsruhe, Deutschland) für 60 Minuten überführt, um unspezifische Proteinbindungen zu blockieren. Es folgte die Verdünnung der Primärantikörper in 1 % PBST und Inkubation bei 4 °C über Nacht. Danach wurden die Proben erneut dreimal mit PBS für 15 Minuten gewaschen. Der fluoreszierende Sekundärantikörper Alexa Fluor 594 goat anti rabbit (Life Technologies, Carlsbad, Vereinigte Staaten von Amerika) wurde mit 1 % BSA in PBST

verdünnt und für 30 Minuten auf die Objektträger gebracht. Danach wurden die Gewebeschnitte einmalig mit PBS für 15 Minuten gespült und schließlich die Zellkerne mit DAPI gefärbt.

2.5) Scoring

Das Scoring basierte auf der visuellen Beurteilung der Zellzahl und der Intensität der Färbung. Die Grade waren: ++: stark positive/positive histochemische Reaktion, mit > 80 % positiver Zellen und/oder hoher Farbintensität; +: schwach positive/teilweise positive Reaktion mit 20 – 80 % positiver Zellen und schwacher oder nur teilweise starker Färbung; -: negative Reaktion mit < 20 % schwach gefärbten Zellen. Des Weiteren wurden bei Bedarf weitere Kommentare angegeben: [1)] stark positiv entweder an der Oberfläche oder in den tiefen Teilen des Tumorgewebes [2)] einzelne Tumorzellen sind stark positiv, aber der Gesamteindruck ist schwach positiv [3)] große Tumorzellen erscheinen stark positiv [4)] teilweise stark positiv [5)] schwach positiv.

3. Ergebnisse

Im Folgenden werden die kombinierte Immunhistochemie- und die Immunfluoreszenz-Daten sowie auch die unterstützenden TMA-Daten für jeden pH-GPCR diskutiert. Die Färbeergebnisse für MM und NZN wurden ferner in epidermale und dermale Anteile unterteilt. Eine Übersicht der Ergebnisse ist in den Abbildungen 5 und 6 gezeigt. Beispielhafte Ergebnisse der Immunhistochemie und –fluoreszenz sind in Abbildung 1-4 dargestellt.

3.1) GPR4 (GPR19)

IHC und IF: 40 % der SCC Gewebeproben zeigten eine starke GPR4-Expression, während 40 % der Proben schwach positiv und 20 % negativ für GPR4 waren (Abb. 1a,e,i). Bezüglich des epidermalen MM-Gewebes exprimierten 20 % der Proben GPR4 stark, 40 % waren schwach oder teilweise positiv und die restlichen 40 % zeigten keine Expression von GPR4. Im Gegensatz dazu waren die dermalen MM Schnitte in 60 % der Proben stark positiv für GPR4 und schwach oder teilweise positiv in 40 % der Fälle (Abb. 2a,e,i, Abb. 5d). 40 % des epidermalen NZN Gewebes zeigte eine stark positive Expression von GPR4, während die restlichen 60 % der Proben schwach oder teilweise positiv waren. Die dermalen Anteile der NZN Gewebeproben zeigten eine ähnliche Verteilung der Expressionsaktivität (Abb. 3a,e,i, Abb. 5c). BCCs exprimierten GPR4 nur in 16,6 % der Fälle stark, während die restlichen 83,3 % der BCCs eine schwache Expression zeigten (Abb. 4a,e,i, Abb. 5b).

Gewebe-Mikroarray (TMA): In den meisten Fällen unterstützte der TMA die Tendenz der vorangegangenen Ergebnisse der kombinierten IHC und IF Daten, mit der Ausnahme von beispielsweise BCC, bei denen in einem Fall keine GPR4 Expression beobachtet wurde. Außerdem wurde GPR4 teilweise weder auf den dermalen Anteilen von NZN noch auf den dermalen Regionen von MM exprimiert, während 94,7% aller untersuchten epidermalen Regionen von MM eine stark positive Expression von GPR4 zeigte.

3.2) TDAG8 (GPR65)

IHC und IF: 20 % der SCC Zellen zeigten eine stark positive Expression, 80 % schienen TDAG8 schwächer oder nur teilweise zu exprimieren (Abb. 1b,f,j, Abb. 5a). 60 % der epidermalen Teile von MM zeigten eine starke und 40 % eine schwach positive TDAG8 Expression, während 60 % der dermalen Regionen von MM schwach positiv waren und 40 % zeigten überhaupt keine Expression (Abb. 2b,f,j, Abb. 5d). 40 % der epidermalen NZN Schnitte zeigten eine stark positive Expression von TDAG8. Die anderen 60 % zeigten eine schwach positive Expression. Das Auftreten von TDAG8 im dermalen Anteil von NZN war dem im epidermalen Anteil ähnlich (Abb. 3b,f,j, Abb. 5c). Das BCC (Abb. 4b,f,j, Abb. 5b) zeigte eine stark positive Färbung von TDAG8 in 33,3 % der Fälle, 33,3 % der Zellen waren schwach positiv und 33,3 % negativ für TDAG8.

TMA: Insgesamt stimmte der Gewebe-Mikroarray mit den vorherigen Ergebnissen weitgehend überein. Die Auswertung der TMAs für TDAG8 ergab allerdings, dass im Gegensatz zu den IHC/IF-Ergebnissen, alle BCC keine TDAG8 exprimierten und 69,6 % der dermalen Regionen von MM eine stark positive Expression zeigten.

3.3) OGR1 (GPR68)

IHC und IF: 20 % der Gewebeproben von SCC waren schwach positiv für OGR1, während die anderen 80 % keine Expression von OGR1 zeigten (Abb. 1c,g,k, Abb. 5a). 40 % der epidermalen Gewebeproben von MM exprimierten OGR1 stark, 40 % waren schwach positiv und die anderen 20 % waren negativ für OGR1. Demgegenüber zeigten 80 % der dermalen Bereiche von MM eine teilweise oder schwach positive Expression und 20 % zeigten eine stark positive Expression (Abb. 2c,g,k, Abb. 5d). 60 % der epidermalen Gewebeproben von NZN waren schwach positiv und die anderen 40 % exprimierten OGR1 stark. Dermale Bereiche in NZN Gewebeproben zeigten eine starke Expression in 20 % der Fälle, in 60 % eine teilweise Expression und keine Expression in 20 % der getesteten Proben (Abb. 3c,g,k, Abb. 5c). 33,3 %

der Proben von BCC (Abb. 4c,g,k, Abb. 5b) waren schwach positiv und die anderen 66,6 % waren negativ für OGR1.

TMA: Zusammengenommen korreliert der TMA mit den Ergebnissen des IHC/IF mit Ausnahme bei den BCC und den epidermalen Anteilen der NZN: 75 % der Proben von BCC zeigten eine partiell oder schwach positive Expression von OGR1 und 64,3 % der epidermalen Anteile von NZN waren negativ für OGR1. Zudem soll erwähnt sein, dass SCC, die dermalen Anteile von NZN und die epidermalen Regionen von MM anteilig mehr positive Einzelscores aufwiesen als die IHC/F-Ergebnisse.

3.4) G2A (GPR132)

IHC und IF: 40 % der SCC Gewebeproben zeigten eine deutlich positive Expression von G2A (GPR132), 40 % schienen schwach oder teilweise positiv zu sein und die anderen 20 % zeigten keine Expression von G2A (Abb. 1d,h,l, Abb. 5a). In 20 % der Proben zeigten die epidermalen Abschnitte von MM eine stark und in 60 % eine schwach positive Expression von G2A. In 20 % der Fälle gab es keine Expression von G2A. In den dermalen Bereichen von MM exprimierten 20 % G2A stark, während 80 % eine schwach positive Expression zeigten (Abb. 2d,h,l, Abb. 5d). Beide NZN Anteile, sowohl epidermal als auch dermal, lieferten entweder stark oder teilweise schwach positive Ergebnisse: 40 % der NZN Proben waren stark positiv und 60 % waren schwach positiv innerhalb der epidermalen Anteile von NZN. Im Fall der dermalen Region von NZN waren die Ergebnisse genau umgekehrt: 60 % zeigten eine stark positive G2A Expression, aber nur 40 % waren schwach positiv (Abb. 3d,h,l, Abb. 5c). Bezüglich der Expression von G2A auf BCC Zellen (Abb. 4d,h,l, Abb. 5b) exprimierten etwa 50 % der Gewebeproben G2A stark und 50 % waren teilweise positiv.

TMA: Größtenteils bestätigten die TMA-Ergebnisse die IHC/IF–Ergebnisse. Geringe Abweichungen waren lediglich beim NZN und der epidermalen Region von MM zu beobachten.

4. Zusammenfassung

In dieser Studie haben wir die Expressionsprofile der pH-GPCRs GPR4 (GPR19), TDAG8 (GPR65), OGR1 (GPR68) und G2A (GPR132) bei verschiedenen Arten von häufig vorkommenden Hauttumoren, SCC, MM, NZN und BCC, untersucht.

Jeder Tumor exprimiert typische Gruppen von pH-GPCRs: (1) SCC exprimiert TDAG8 stark (IHC: Abb. 5a, TMA: Abb. 6a) und zeigt keine Expression (IHC: Abb. 5a) bzw. eine moderate Expression (TMA: Abb. 6a) von OGR1. (2) MM exprimiert TDAG8 stark epidermal (IHC:

Abb. 5d, TMA: Abb. 6d) sowie GPR4, OGR1 und G2A (alle TMA: Abb. 6d) stark dermal. (3) Insgesamt exprimieren NZN GPR4, TDAG8 und G2A moderat bis stark positiv epidermal (IHC: Abb. 5c, TMA: Abb. 6c) sowie TDAG8 stark dermal (IHC: Abb. 5c, TMA: Abb. 6c). (4) BCC exprimiert GPR4 (IHC: Abb. 5b) sowie G2A (IHC: Abb. 5b, TMA: Abb. 6b) stark und zeigt keine Expression von OGR1 (IHC: Abb. 5b). Es ist auffällig, dass alle vier GPCRs besonders häufig in NZN und MM exprimiert sind. Jede weitere Kombination von Rezeptor und Tumortyp ergab uneinheitliche Ergebnisse.

Die durchaus inhomogenen Expressionsprofile unterstützen das aktuelle Wissen über die teils gegensätzlichen Rollen der vier pH-GPCRs innerhalb eines Tumors.[13,20]

Während GPR4 nur schwach auf den dermalen Anteilen von NZN, SCC, BCC exprimiert wurde (IHC: Abb. 5 a,b, TMA: Abb. 6 a,c), zeigten die untersuchten dermalen Bereiche von MM eine stark positive Expression von GPR4: Interessanterweise zeigte die TMA Technologie eine starke Expression von GPR4 in den epidermalen Abschnitten von MM (TMA: Abb. 6d) und IHC/IF unterstützte dieses Ergebnis mit einer ebenfalls stark positiven Expression von GPR4 in den epidermalen Regionen mit Ausnahme von zwei der insgesamt fünf entnommenen Gewebeproben (IHC: Abb. 5d).

GPR4-defiziente Mäuse zeigten eine signifikant reduzierte angiogene Reaktion auf VEGF, welches zu einer Reduktion des Tumorwachstums in den orthotopischen Maus-Modellen führte.[21] Im Gegensatz dazu hemmte eine GPR4-Überexpression und die Herstellung eines sauren pH-Wertes, die Migration, Invasion und Metastasenbildung von B16F10 Melanomzellen.[22] Mit Hinblick auf unsere Ergebnisse könnte GPR4 ein Indikator für Dysplasien von dermalen Melanozyten sein, ähnlich wie HMB45.[23] Letzteres bleibt auch häufig in den tiefen dermalen Anteilen von dysplastischen Nävi oder dem Melanom positiv, während Expressionsaktivitäten mit zunehmender Tiefe im normalen Nävi abnehmen. In unseren Studien zeigte sich eine erhöhte GPR4 Expression in dermalen Bereichen der MM im Vergleich zu dermalen NZN Bereichen. Nach TMA-Ergebnissen wurde GPR4 auch in den epidermalen Bereichen in MM starker exprimiert als in NZN.

In allen vier untersuchten Tumortypen war die Expression von TDAG8 stark positiv (TMA: Abb. 6a, 6c, 6d), ausgenommen die dermalen Anteile von MM (IHC: Abb. 5d), die epidermalen Bereichen von NZN (TMA: Abb. 6c) und BCC (IHC: Abb. 5b) zeigten eine schwach positive oder sogar fehlende Expression von TDAG8. Eine Überexpression von TDAG8 in Lungenkarzinomzellen wurde mit einer verstärkten Tumorentwicklung und dem Überleben von Krebszellen unter sauren Bedingungen assoziiert.[24] Auf der anderen Seite erhöhte eine Überexpression des TDAG8-GFP Fusionsproteins in Lymphomzellen deren

Sensibilität gegenüber Dexamethason-induzierter Apoptose.[25] Daher kann man spekulieren, dass die hohe Expression von TDAG8 in den hier untersuchten Haut-Tumoren entscheidend für das Wachstum und/oder das Überleben von Tumorzellen sein könnten. Alternativ könnte TDAG8 zur Kontrolle des Tumorwachstums unter sauren Bedingungen und somit als Tumor-suppressiver Rezeptor wirken.

OGR1 wurde weder auf dem SCC (IHC: Abb. 5a) noch auf dem BCC (IHC: Abb. 5b) exprimiert, allerdings wurde eine partielle Expression auf MM und NZN beobachtet (IHC: Abb. 5c,d, TMA: 6c,d). Es wurde gezeigt, dass die OGR1-Überexpression in Eierstockkrebszellen die Tumorzellmigration hemmt und von einem Anstieg der Zell-Matrix-Adhäsion begleitet wird.[26] Obwohl dies zunächst auf eine Tumor-suppressive Wirkung hindeutet, weisen andere Beobachtungen eher auf eine Tumor-promovierende Funktion von OGR1 im Wirtsorganismus hin. Ein Mangel an OGR1 in den Wirtszellen von Knockoutmäusen beeinträchtigte beispielsweise die Tumorgenese von Melanomzellen und Prostatakrebszellen.[27,28] Eine Expression von ORG1 kann demnach gegensätzliche Funktionen haben, je nachdem ob der pH-GPCR von Zellen des Tumors oder Zellen des Wirtsorganismus exprimiert wird. Dies könnte einen Erklärungsansatz für die hohe Expression von OGR1 in den mesenchymalen Tumoren NZN und MM im Gegensatz zur moderaten Expression in den epithelialen Tumoren SCC und BCC liefern. Weitere Experimente sind erforderlich, um die eventuell bestehenden Zusammenhänge besser zu verstehen.

Die Expression von G2A in den untersuchten Tumoren war sowohl in den epidermalen als auch dermalen Anteilen von MM, NZN und BCC hoch (IHC: Abb. 5b,c, TMA: Abb. 6b,d). Demgegenüber zeigte SCC auch vereinzelt eine negative Expression (IHC: Abb. 5a). G2A wird eine wichtige Rolle in der Kontrolle der Homöostase von Immunzellen zugesprochen. Dies wird durch die Feststellung unterstützt, dass ein G2A-Defizit Autoimmunerkrankungen in alternden G2A–Knockoutmäusen verursacht.[29] Die Expression von G2A in anderen Zelltypen scheint jedoch ein onkogenes Potenzial zu haben.[30] In menschlichen epidermalen Keratinozyten vermittelt G2A die Sekretion von Zytokinen und veranlasst den Stillstand des Zellzyklus.[31] UVB-Strahlung und H_2O_2 verstärken die G2A-Expression in HaCaT-Zellen, was darauf hinweist, dass G2A als Sensor für DNA-Schäden und oxidativen Stress in Keratinozyten fungieren könnte.[32] Aufgrund seiner hohen Expression in den Hauttumoren MM, NZN, SCC und BCC, könnte G2A als entscheidender Immunkontrollpunkt des Tumors fungieren, was allerdings weiteren Untersuchungen bedarf.

Die TMA-Resultate lassen erkennen, dass die Gesamtexpression aller vier GPCRs in MM im Vergleich zu NZN zunimmt. Daher suggerieren die Ergebnisse, dass ein Anstieg der pH-GPCR

Expression in MM, ein Marker für eine erhöhte Malignität sein könnte, was jedoch weitere Untersuchungen fordert.

Somit liefern unsere Untersuchungen viele Ansatzpunkte für spezifische Fragestellungen zur Rolle der vier pH-GPCRs in typischen Hauttumoren, die beispielsweise mit Hilfe von gezielten Zellkulturstudien verfolgt werden können. Zu Grunde liegende Ergebnisse und nachfolgende Studien können somit zur Aufklärung der Rolle von pH-GPCRs in verschiedenen Hauttumoren und einer potentiellen Verwendung als therapeutisches Target führen.

5. Literaturverzeichnis

1. Apalla Z, Nashan D, Weller RB, Castellsagué X. Skin Cancer: Epidemiology, Disease Burden, Pathophysiology, Diagnosis, and Therapeutic Approaches. *Dermatol Ther*. 2017;7(Suppl 1):5-19.
2. Augustin J, Kis A, Sorbe C, Schäfer I, Augustin M. Epidemiology of skin cancer in the German population: impact of socioeconomic and geographic factors. *J Eur Acad Dermatol Venereol*. 2018;32(11):1906-1913.
3. Hanlon, A. Metastatic Squamous Cell Carcinoma: Epidemiology and Available Systemic Therapies. *Curr Derm Rep 2*. 2013;118-124.
4. Mackiewicz-Wysocka M, Bowszyc-Dmochowska M, Strzelecka-Węklar D, Dańczak Pazdrowska A, Adamski Z. Basal cell carcinoma - diagnosis. *Contemp Oncol*. 2013;17(4):337-342.
5. Viana AC, Gontijo B, Bittencourt FV. Giant congenital melanocytic nevus. *An Bras Dermatol*. 2013;88(6):863-878.
6. Damsky WE, Bosenberg M. Melanocytic nevi and melanoma: unraveling a complex relationship. *Oncogene*. 2017;36(42):5771-5792.
7. Linares MA, Zakaria A, Nizran P. Skin Cancer. *Prim Care*. 2015;42(4):645-659.
8. Zbytek B, Carlson JA, Granese J, Ross J, Mihm MC Jr, Slominski A. Current concepts of metastasis in melanoma. *Expert Rev Dermatol*. 2008;3(5):569-585.
9. Graul RC, Sadée W. Evolutionary relationships among G protein-coupled receptors using a clustered database approach. *AAPS Pharm Sci*. 2001;3(2):E12.
10. Lee HJ, Wall B, Chen S. G-protein-coupled receptors and melanoma. *Pigment Cell Melanoma Res*. 2008;21(4):415-428.
11. Ludwig MG, Vanek M, Guerini D, et al. Proton-sensing G-protein-coupled receptors. *Nature.* 2003;425(6953):93-98.
12. Justus CR, Dong L, Yang LV. Acidic tumor microenvironment and pH-sensing G protein-coupled receptors. *Front Physiol*. 2013;4:354.
13. Weiss KT, Fante M, Kohl G, et al. Proton-sensing G protein-coupled receptors as regulators of cell proliferation and migration during tumor growth and wound healing. *Exp Dermatol.* 2017;26(2):127-132.
14. Neri D, Supuran CT. Interfering with pH regulation in tumours as a therapeutic strategy. *Nat Rev Drug Discov.* 2011;10(10):767-777.
15. Tomura H, Mogi C, Sato K, Okajima F. Proton-sensing and lysolipid-sensitive G-protein coupled receptors: a novel type of multi-functional receptors. *Cell Signal.* 2005;17(12):1466-1476.
16. Webb BA, Chimenti M, Jacobson MP, Barber DL. Dysregulated pH: a perfect storm for cancer progression. *Nat Rev Cancer.* 2011;11(9):671-677.
17. Im D-S. Orphan G Protein Coupled Receptors and Beyond.pdf. *Jpn J Pharmacol.* 2002;90:101-106.
18. Cardone RA, Casavola V, Reshkin SJ. The role of disturbed pH dynamics and the Na+/H+ exchanger in metastasis. *Nat Rev Cancer.* 2005;5(10):786-795.

19. Haverkampf S, Heider J, Weiß KT, et al. NHE1 expression at wound margins increases time-dependently during physiological healing. *Exp Dermatol*. 2017;26(2):124-126.
20. Nassios A, Wallner S, Haferkamp S, Klingelhöffer C, Brochhausen C, Schreml S. Expression of proton-sensing G-protein-coupled receptors in selected skin tumors. *Exp Dermatol*. 2019;28(1):66-71.
21. Wyder L, Suply T, Ricoux B, et al. Reduced pathological angiogenesis and tumor growth in mice lacking GPR4, a proton sensing receptor. *Angiogenesis*. 2011;14(4):533-544.
22. Castellone RD, Leffler NR, Dong L, Yang LV. Inhibition of tumor cell migration and metastasis by the proton-sensing GPR4 receptor. *Cancer Lett.* 2011;312(2):197-208.
23. Ohsie SJ, Sarantopoulos GP, Cochran AJ, Binder SW. Immunohistochemical characteristics of melanoma. *J Cutan Pathol*. 2008;35(5):433-444.
24. Ihara Y, Kihara Y, Hamano F, et al. The G protein-coupled receptor T-cell death-associated gene 8 (TDAG8) facilitates tumor development by serving as an extracellular pH sensor. *Proc Natl Acad Sci U S A*. 2010;107(40):17309- 17314.
25. Malone MH, Wang Z, Distelhorst CW. The glucocorticoid-induced gene tdag8 encodes a pro-apoptotic G protein-coupled receptor whose activation promotes glucocorticoid-induced apoptosis. *J Biol Chem.* 2004;279(51):52850-52859.
26. Ren J, Zhang L. Effects of ovarian cancer G protein coupled receptor 1 on the proliferation, migration, and adhesion of human ovarian cancer cells. *Chin Med J (Engl)*. 2011;124(9):1327-1332.
27. Li H, Wang D, Singh LS, et al. Correction: abnormalities in osteoclastogenesis and decreased tumorigenesis in mice deficient for ovarian cancer g protein-coupled receptor 1. *PLoS One*. 2015;10(4):e0125463.
28. Yan L, Singh LS, Zhang L, Xu Y. Role of OGR1 in myeloid-derived cells in prostate cancer. *Oncogene*. 2014;33(2):157-164.
29. Le LQ, Kabarowski JH, Weng Z, et al. Mice lacking the orphan G protein-coupled receptor G2A develop a late-onset autoimmune syndrome. *Immunity*. 2001;14(5):561-571.
30. Zohn IE, Klinger M, Karp X, et al. G2A is an oncogenic G protein-coupled receptor. *Oncogene*. 2000;19(34):3866-3877.
31. Obinata H, Izumi T. G2A as a receptor for oxidized free fatty acids. *Prostaglandins Other Lipid Mediat*. 2009;89(3-4):66-72.
32. Hattori T, Obinata H, Ogawa A, et al. G2A plays proinflammatory roles in human keratinocytes under oxidative stress as a receptor for 9-hydroxyoctadecadienoic acid. *J Invest Dermatol*. 2008;128(5):1123-1133.

6. Anhang

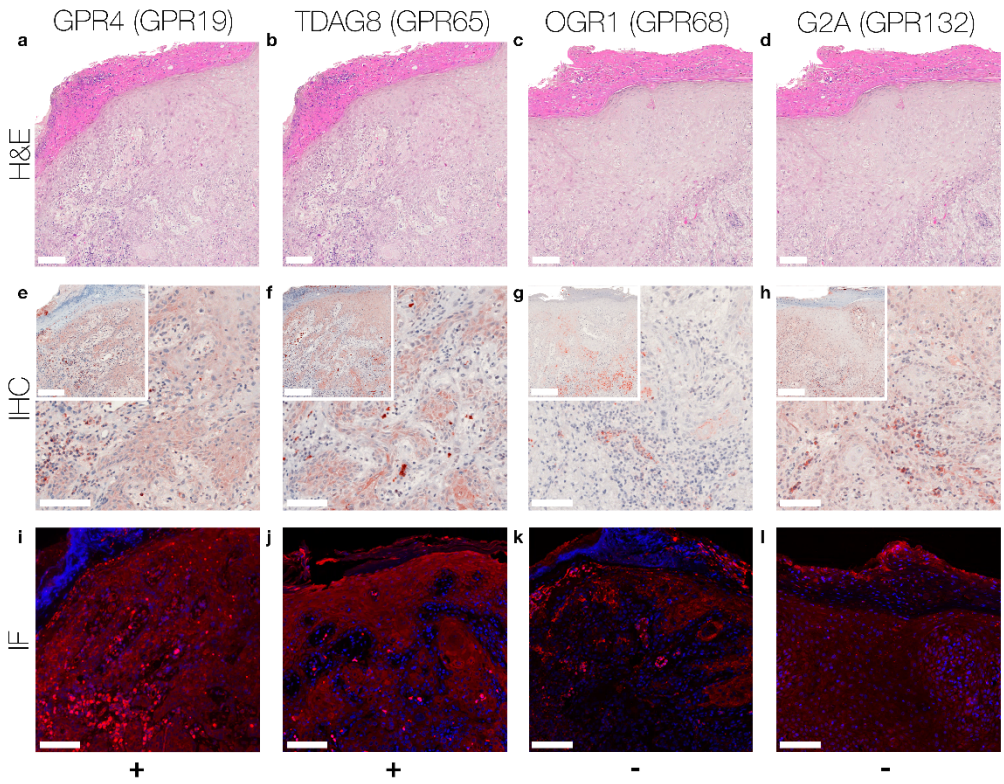

Abbildung 1: Immunhistochemie und Immunfluoreszenz SCC.

Immunhistochemische und immunfluoreszente Färbungen für GPR4, GPR65, GPR68 und GPR132 an SCC Geweben. (a-d) Histochemische H&E Färbung, (e-h) immunhistochemische Färbung, eingefügte Bilder zeigen ein 2x vergrößertes Sichtfeld (i-l), immunfluoreszente Färbung, rot: Antikörpermarkierung, blau: DAPI. Maßstabsbalken entsprechen 100 µm (a-l: Patient 1). Scores (unterste Reihe) wurden vergeben für ++: stark positive/ positive Reaktionen; +: schwach positive/teilweise positive Reaktionen; -: negative Reaktionen. Dieses SCC zeigt keine Expression von OGR1 und G2A, jedoch erscheinen einzelne peritumoröse gelegene Lymphozyten positiv.

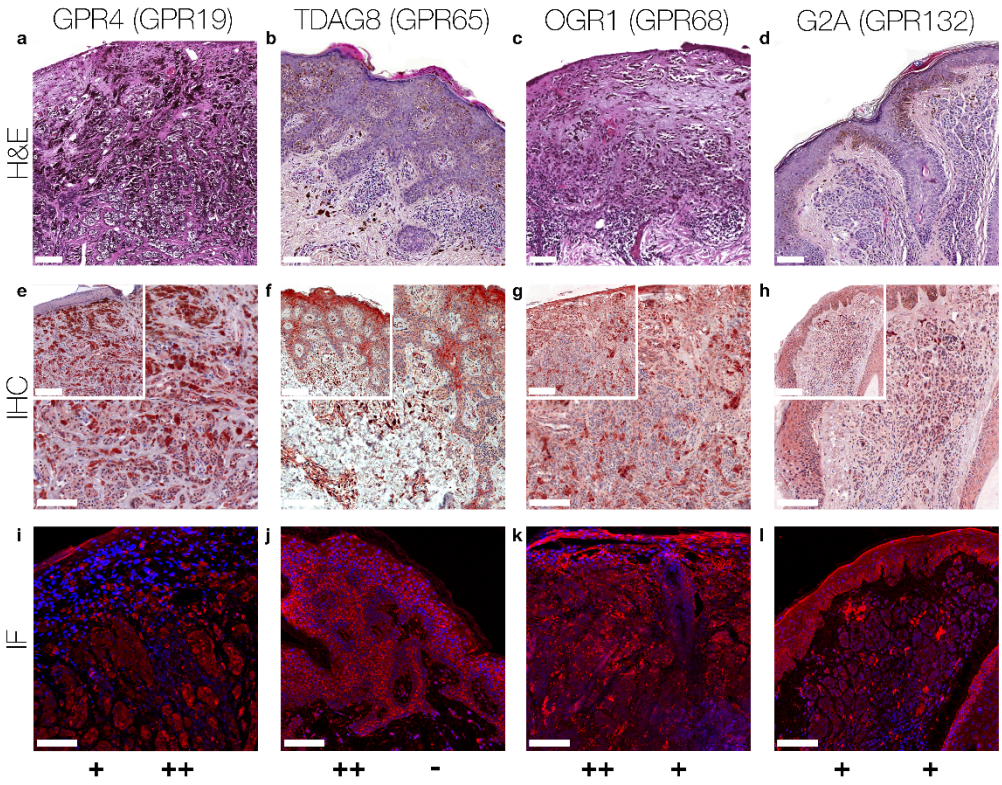

Abbildung 2: Immunhistochemie und Immunfluoreszenz MM.

Immunhistochemische und immunfluoreszente Färbung für GPR4, GPR65, GPR68 und GPR132 an Gewebeschnitten des MM. (a-d) Histochemische H&E Färbung, (e-h) immunhistochemische Färbung, eingefügte Bilder zeigen ein 2x vergrößertes Sichtfeld (i-l), immunfluoreszente Färbung, rot: Antikörpermarkierung, blau: DAPI. Maßstabsbalken entsprechen 100 µm (a, c, e, g, i, k: Patient 8; b, d, f, h, j, l: Patient 9). Scores (unterste Reihe) wurden vergeben für ++: stark positive/ positive Reaktionen; +: schwach positive/teilweise positive Reaktionen; -: negative Reaktionen für Epidermis (linker Score) und die Dermis (rechter Score). Dieses MM zeigt eine stark positive Expression von TDAG8 und OGR1 in den epidermalen Anteilen. Die epidermale Expression von GPR4 und G2A erscheint partiell positiv. Es gibt eine stark positive dermale Expression von GPR4. OGR1 und G2A sind in Bezug auf die Dermis schwach positiv ausgeprägt und TDAG8 wird dermal nicht exprimiert. Im Allgemeinen, erscheinen kleinere Tumorzellen innerhalb des Tumors schwach positiv, während unterhalb der Epidermis mehrkernige Riesentumorzellen mit einem veränderten Kern-Plasma Relation stark exprimiert werden.

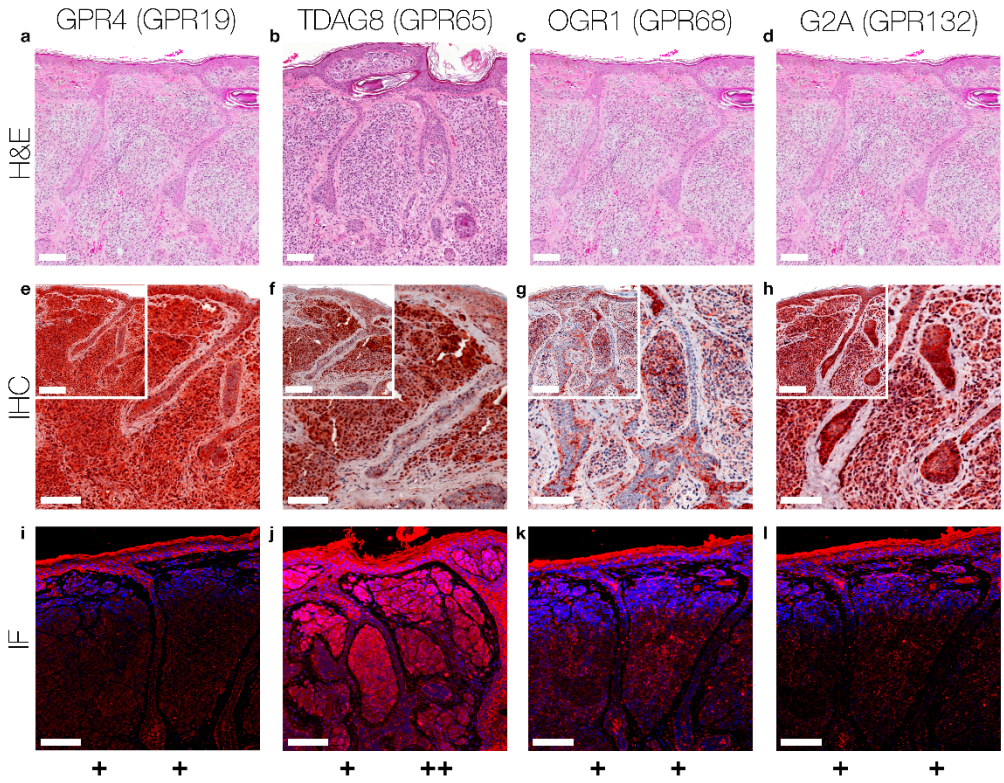

Abbildung 3: Immunhistochemie und Immunfluoreszenz NZN.

Immunhistochemische und immunfluoreszente Färbung für GPR4, GPR65, GPR68 und GPR132 an NZN Geweben. (a-d) Histochemische H&E Färbung, (e-h) immunhistochemische Färbung, eingefügte Bilder zeigen ein 2x vergrößertes Sichtfeld, (i-l) immunfluoreszente Färbung, rot: Antikörpermarkierung, blau: DAPI. Maßstabsbalken entsprechen 100 µm (a-l: patient 15). Scores (unterste Reihe) wurden vergeben für ++: stark positive/ positive Reaktionen; +: schwach positive/teilweise positive Reaktionen; -: negative Reaktionen für Epidermis (linker Score) und die Dermis (rechter Score). Dieses NZN zeigt eine partiell positive Expression aller GPCRs auf den epidermalen Anteilen. Es gibt sogar einige epidermale Tumorzellen, die stark von TDAG8 exprimiert werden. In Bezug auf die Dermis von GPR4, OGR1 und G2A sind diese schwach positiv ausgeprägt, während MM eine signifikant gesteigerte Expression von TDAG8 zeigt.

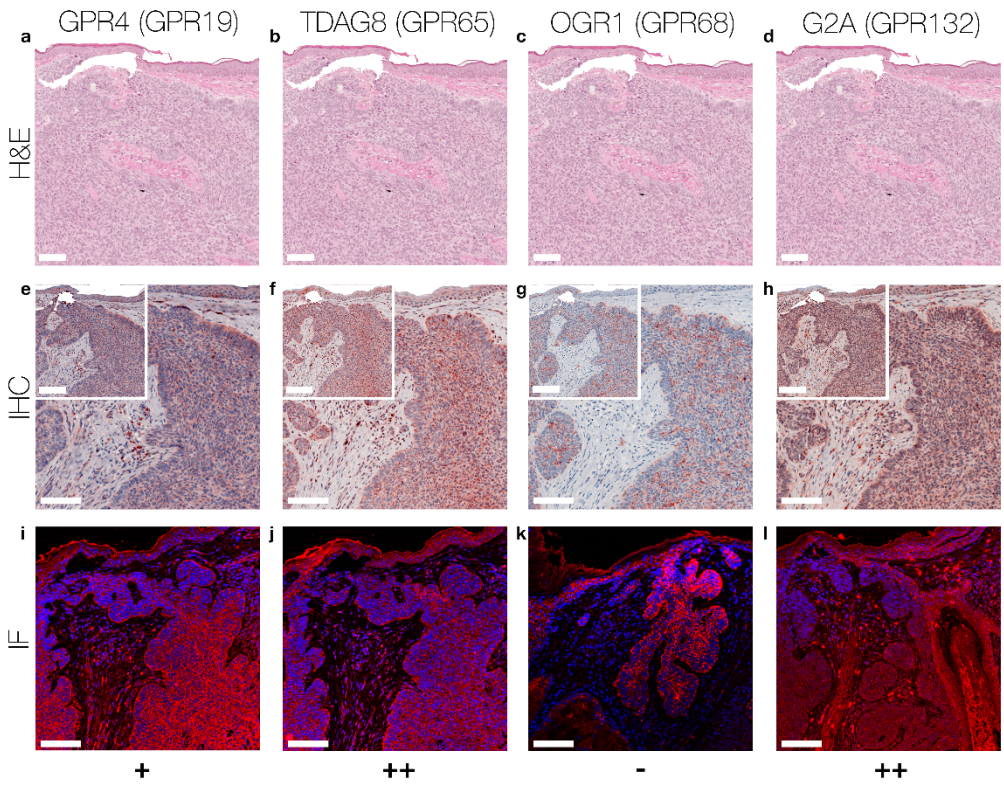

Abbildung 4: Immunhistochemie und Immunfluoreszenz BCC.

Immunhistochemische und immunfluoreszente Färbung für GPR4, GPR65, GPR68 und GPR132 an Gewebeschnitten von BCC. (a-d) Histochemische H&E Färbung, (e-h) immunhistochemische Färbung, eingefügte Bilder zeigen ein 2x vergrößertes Sichtfeld (i-l), immunfluoreszente Färbung, rot: Antikörpermarkierung, blau: DAPI. Maßstabsbalken entsprechen 100 µm (a-l: Patient 20). Scores (unterste Reihe) wurden vergeben für ++: stark positive/ positive Reaktionen; +: schwach positive/teilweise positive Reaktionen; -: negative Reaktionen. Die Expression von TDAG8 und G2A auf der Oberfläche der BCC-Tumorzellen ist signifikant gesteigert, während die Expression von GPR4 schwach positiv ist. Es zeigt keine Expression von OGR1.

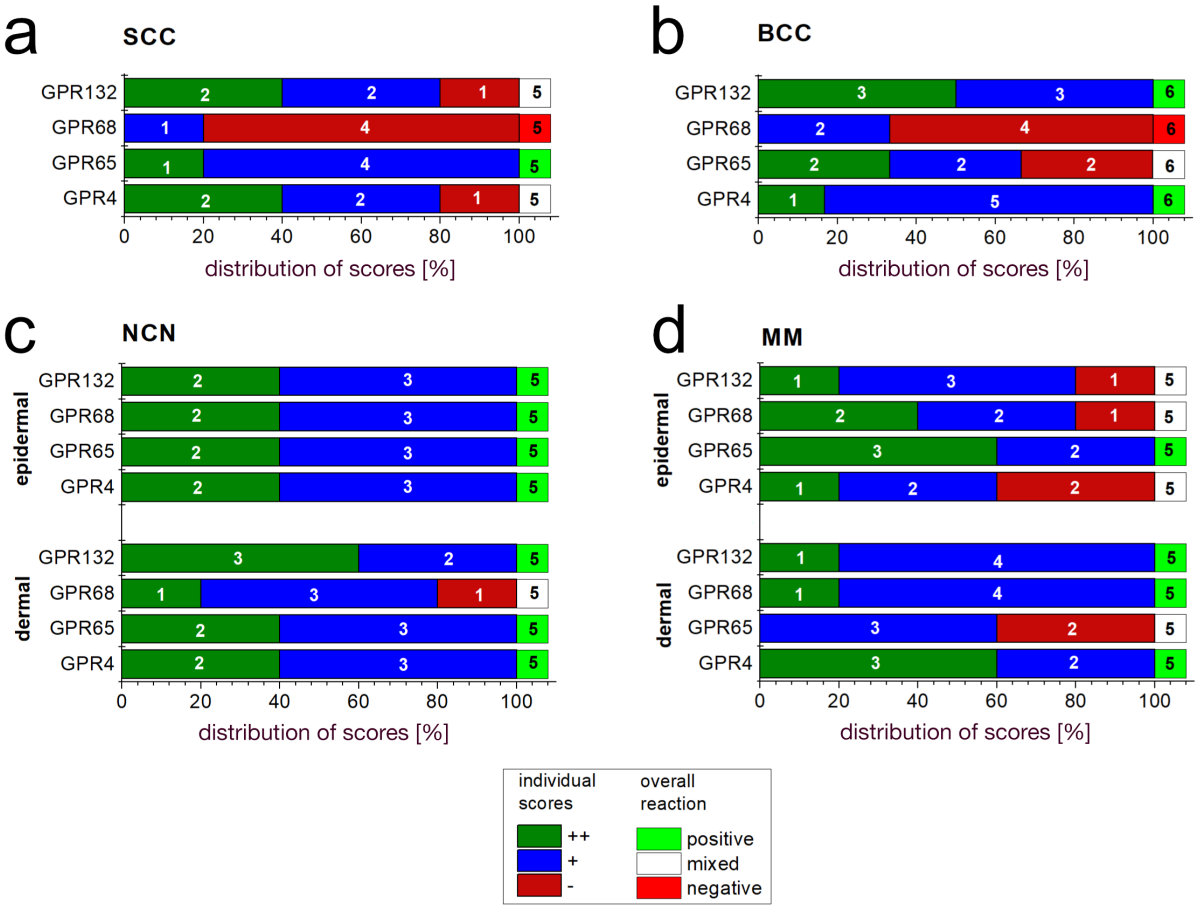

Abbildung 5: Zusammenfassung der Ergebnisse für Immunhistochemie und Immunofluoreszenz von Protonen-sensitiven GPCRs auf häufig vorkommenden Hauttumoren: Verteilung der Scores von immunhistochemischen und immunofluoreszenten Färbungen (grüner Balken, ++: stark positive / positive Reaktion; +, blauer Balken: schwach positive/ partiell positive Reaktion; -, roter Balken: negative Reaktion) für GPR4 (GPR19), TDAG8 (GPR65), OGR1 (GPR68) und G2A (GPR132) auf (a) SCC, (b) BCC, (c) NZN, (d) MM. MM und NZN werden zudem weiter unterteilt in epidermale und dermale Anteile. Die Zahlen in den Balken geben das Auftreten einer entsprechenden Punktzahl an. Die Summe aller Punkte ist 100%. Die Gesamtbewertung wird durch ein grünes, weißes oder rotes Kästchen angezeigt: grüne Box: insgesamt positive Reaktionen; rote Box: insgesamt negative Reaktionen; weiße Box: uneinheitliche Reaktionen. Die Zahlen in diesen Feldern ergeben die Gesamtzahl der untersuchten Proben an.

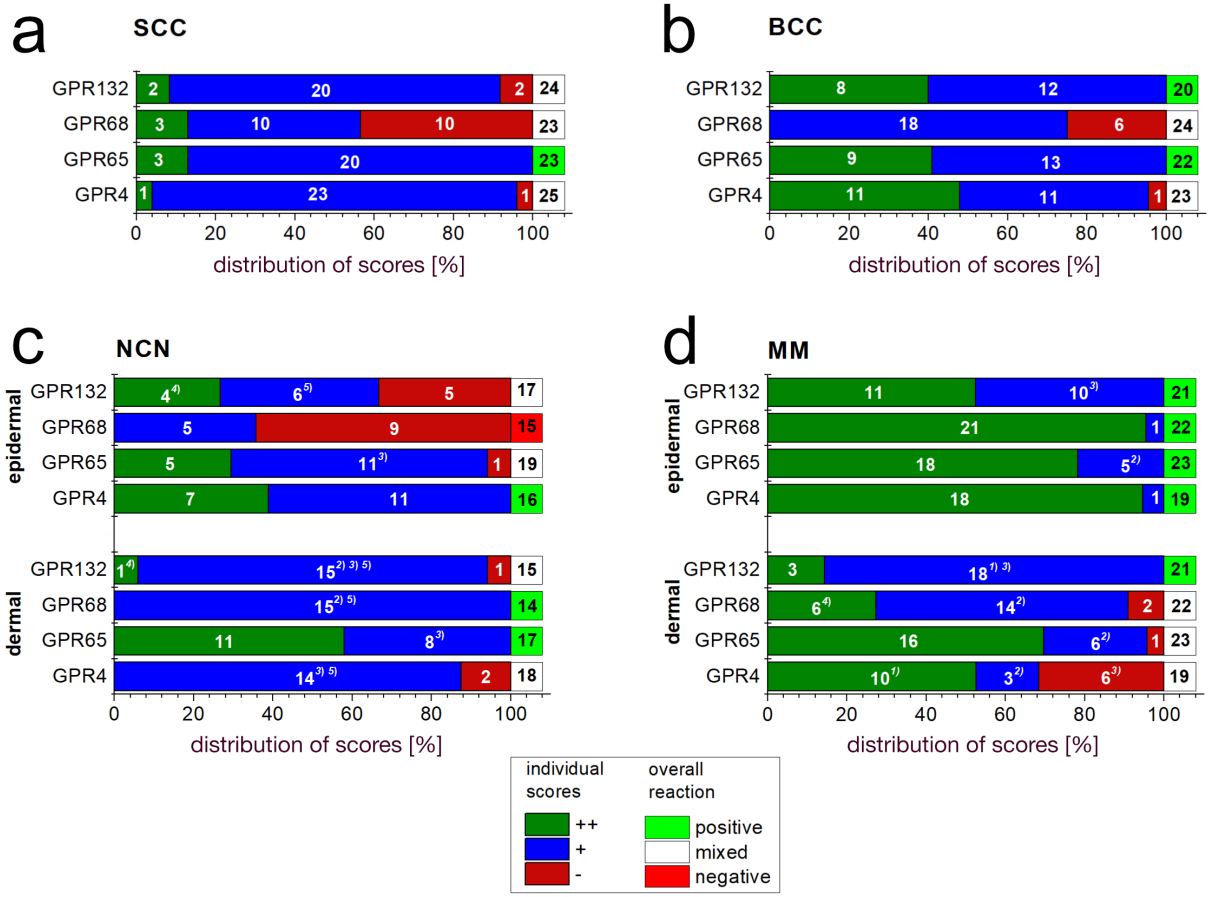

Abbildung 6: Zusammenfassung der Scores von Gewebe-Mikroarray (TMA) von Protonen-sensitiven GPCRs auf häufig vorkommenden Hauttumoren: Verteilung der Scores von immunhistochemischen und immunofluoreszenten Färbungen (grüner Balken, ++: stark positive / positive Reaktion; +, blauer Balken: schwach positive/ partiell positive Reaktion; -, roter Balken: negative Reaktion) für GPR4 (GPR19), TDAG8 (GPR65), OGR1 (GPR68) und G2A (GPR132) auf (a) SCC, (b) BCC, (c) NZN, (d) MM. MM und NZN werden zudem weiter unterteilt in epidermale und dermale Anteile. Die Zahlen in den Balken geben das Auftreten einer entsprechenden Punktzahl an. Die Summe aller Punkte ist 100%. Die Gesamtbewertung wird durch ein grünes, weißes oder rotes Kästchen angezeigt: grüne Box: insgesamt positive Reaktionen; rote Box: insgesamt negative Reaktionen; weiße Box: uneinheitliche Reaktionen. Die Zahlen in diesen Feldern geben die Gesamtzahl der untersuchten Proben an.

SCIENTIFIC REPORTS
nature research

OPEN

Expression profiles of proton-sensing G-protein coupled receptors in common skin tumors

Wybke Klatt[1], Susanne Wallner[1], Christoph Brochhausen[2], Judith A. Stolwijk[1,3,4] & Stephan Schreml[1,4]✉

The proton-sensing GPCRs (pH-GPCRs) GPR4 (GPR19), TDAG8 (GPR65, T-cell death associated gene 8), OGR1 (GPR68, ovarian cancer GPCR1), and G2A (GPR132, G2 accumulation protein) are involved in sensing and transducing changes in extracellular pH (pH_e). Extracellular acidification is a central hallmark of solid cancer. pH-GPCR function has been associated with cancer cell proliferation, adhesion, migration and metastasis, as well as with modulation of the immune system. Little is known about the expression levels and role of pH-GPCRs in skin cancer. To better understand the functions of pH-GPCRs in skin cancer in vivo, we examined the expression-profiles of GPR4, TDAG8, OGR1 and G2A in four common skin tumors, i.e. squamous cell carcinoma (SCC), malignant melanoma (MM), compound nevus cell nevi (NCN), basal cell carcinoma (BCC). We performed immunohistochemistry and immunofluorescence staining on paraffin-embedded tissue samples acquired from patients suffering from SCC, MM, NCN or BCC. We show the expression of pH-GPCRs in four common skin cancers. Different expression patterns in the investigated skin cancer types indicate that the different pH-GPCRs may have distinct functions in tumor progression and serve as novel therapeutic targets.

In 2019, the United States are projecting 1,762,450 new cancer cases to occur[1]. Over the past decade particularly skin cancer, one of the most common types of malignancies, has shown an increasing incidence[2,3]. Among non-melanoma skin cancers, squamous cell carcinoma (SCC) grows slow over months and only 4% of the SCC tumours metastasise, leading to significant patient morbidity[4]. SCC is the second most-frequent cutaneous malignancy, preceded in frequency by the basal cell carcinoma (BCC). BCC is characterised by a slow growing behaviour and metastases are extremely rare[5]. Nevus cell nevi (NCN) are benign melanocytic lesions which do not require any intervention[6]. The malignant melanoma (MM) develops from the nevus cell nevus in one third of the cases[7]. Although MM represents only 2% of the malignant skin cancer incidents, it is still one of the deadliest skin cancers with a rapid systematic dissemination[8,9].

G-protein coupled receptors (GPCRs) are one of the most diverse classes of cell surface receptors with over 500 representatives in eukaryotes, including animals, plants, fungi and the human body, where they fulfil a multitude of crucial individual tasks[10,11].

The pH-sensitive GPCRs (pH-GPCRs) GPR4 (GPR19), TDAG8 (GPR65, T-cell death associated gene 8), OGR1 (GPR68, ovarian cancer GPCR1) and G2A (GPR132, G2 accumulation protein) are activated by protons in the extracellular environment, presumably through binding to specific histidine residues at the extracellular surface of these receptors[12]. Under healthy conditions the central function of these proton sensors seems the maintenance of homeostasis. However, in tumours it is believed that certain pH-GPCRs may help to establish a growth advantage while others inhibit growth[13,14]. Moreover, there are differences between the tumor types[15].

Tumor pH often differs from normal tissue. While standard stromal cells maintain intracellular pH (pH_i) in a narrow range of 6.9–7.2 compared to the extracellular pH (pH_e) of 7.2–7.4, tumors exhibit lower pH_e (6.2–7.0)

[1]Department of Dermatology, University Medical Center Regensburg, Franz-Josef-Strauß-Allee 11, 93053 Regensburg, Germany. [2]Institute of Pathology, University of Regensburg, Franz-Josef-Strauß-Allee 11, 93053 Regensburg, Germany. [3]Institute of Analytical Chemistry, Chemo- and Biosensors, Faculty of Chemistry and Pharmacy, University of Regensburg, Universitätsstraße 31, 93053 Regensburg, Germany. [4]These authors jointly supervised this work: Judith A. Stolwijk and Stephan Schreml. ✉email: stephan@schreml.de

and preserve an alkaline intracellular pH (7.2–7.7)[15,16]. This pH dysregulation, termed reversed (=inside-out) pH gradient ($pH_e < pH_i$), has been recognized as a hallmark of cancer[13,17,18]. The lower pH_e is typically caused by disorganised vascularisation, specific proton transporters and metabolic changes. Insufficient vascularisation leads to the development of hypoxic regions, where instead of aerobic glucose metabolism anaerobic glycolysis takes over, producing lactate[19,20]. In addition, different transporters/pumps are involved in the regulation of tumor pH_i and pH_e, including monocarboxylate transporters 1–4 (MCT), the Na^+/H^+ exchanger 1 (NHE1), HCO_3^- transporters (NBCs), vacuolar ATPases (V-ATPase) as well as different carboanhydrases (CAII, CAIV, CAXII)[12,17–19]. Adaption of cancer cells to extracellular acidosis drives tumor progression by affecting cell turnover, promoting metastasis and metabolic changes[14,17–19,21].

pH-GPCR function has been associated with cancer cell proliferation, adhesion, migration and metastasis, as well as with modulation of the immune system[12,14,22–30], but so far there is no precise concept that links individual pH-GPCR expression to certain cancer cell function.

Only little is known on the expression of proton-sensing GPCRs GPR4, TDAG8, OGR1 and G2A in the skin and especially in skin cancer[15]. The pH-GPCRS GPR4, TDAG8, OGR1, and G2A appear to be expressed in the skin, but data on protein level that clearly link expression to specific skin cells are sparse[14]. Nassios et al.[15] provided first evidence of pH-GPCR expression on protein level in selected rare skin cancers merkel cell carcinoma, dermatofibrosarcoma protuberans, atypical fibroxanthoma and pleomorphic dermal sarcoma.

In this study, we have focussed on analysing the expression levels of the respective pH-GPCRs in tissue samples of four of the most common skin cancer types, SCC, MM, NCN and BCC. The identification of characteristic expression patterns of the four different pH GPCRs in the respective tumour types may help to contribute to a better individual therapy of the four tumour types and enable a more substantial insight into considering pH-GPCRs as therapeutic target.

Results

We summarised our findings of immunohistochemistry data for individual SCC, MM, NCN and BCC tumors from each 5–6 patients. In order to present more data, we performed additional immunohistochemistry on TMA-format including 24–27 samples per tumor type. Figures 1, 2, 3 and 4 show representative IHC and IF staining results on tissue samples with SCC, MM, NCN and BCC for GPR4, TDAG8, OGR1 and G2A. Images from IHC/IF on all other samples can be found in the Supplementary Figures S1–S17. Staining results for MM and NCN were divided in epidermal and dermal portions. Figures 5a–d and 6a–d summarize both, regular IHC and TMA results. General patient information is given in Supplementary Table S1. Additional TMA data and scores are shown in Supplementary Figure S18 and Supplementary Tables S2–S5. In the following the combined immunohistochemistry and immunofluorescence data as well as the supporting TMA data are discussed for each pH-GPCR.

GPR4 (GPR19). *IHC and IF.* According to the IHC data, 40% of the SCC tissue samples showed a strong GPR4 expression, while 40% of the samples were weak positive and 20% negative for GPR4 (Figs. 1a,e,i, 5a and Supplementary Figs. S1–S4 first column). For MM and NCN tumor tissue, epidermal and dermal tumor cells were distinguished in terms of GPR4 expression. Regarding the MM epidermal tissue, 20% of the samples strongly expressed GPR4, 40% were weak or partial positive and the remaining 40% showed no expression of GPR4. In contrast, the MM dermal sections were strong positive for GPR4 in 60% of the samples and weak or partial positive in 40% of the samples (Figs. 2a,e,i, 5d and Supplementary Figs. S5–S8 first column). 40% of NCN epidermal tissue showed a strong positive expression of GPR4, while the remaining 60% of the samples were only weak or partial positive. The dermal parts of the NCN tissue samples showed similar distribution of expression levels (Figs. 3a,e,i, 5c and Supplementary Figs. S9–S12 first column). BCCs strongly expressed GPR4 in only 16.6% of the cases, while the other 83.3% of BCC showed no expression (Figs. 4a,e,i, 5b and Supplementary Figs. S3–S17 first column).

The tissue microarray analysis (TMA). TMA revealed that while only 4% of the SCC samples were strong positive for GPR4, 92% showed a weak GPR4 expression and 4% were GPR4 negative (Fig. 6a, Fig. S18). MM revealed strong positive results, especially in the epidermal areas of the tissue (94.7%) compared to the dermal section (52.6%) (Fig. 6d). NCN epidermal and dermal parts appeared both weak positive (epidermal: 61.1%, dermal: 87.5%) (Fig. 6c). In the dermal portions of MM and NCN especially the giant tumor cells appeared to be strong positive. 47.8% of BCC tissue samples strongly expressed GPR4 (Fig. 6b). Other TMA BCC tissue exhibited a weak positive expression (47.8%) or were negative for GPR4 (4.4%). For most instances, the TMA supported the trend of results described for the combined IHC and IF data, except of the BCC where one case not expressing GPR4 was observed in the TMA.

TDAG8 (GPR65). *IHC and IF.* Regarding the expression-profile of TDAG8 (GPR65), 20% of the SCC cells showed a strong positive expression, 80% seemed to express TDAG8 weaker or only partial (Figs. 1b,f,j, 5a and Supplementary Figs. S1–S4 second column). 60% of the MM epidermal sections showed a strong and 40% a weak TDAG8 expression, whereas 60% of the MM dermal sections were weak positive and 40% showed no expression at all (Figs. 2b,f,j, 5d and Supplementary Figs. S5–S8 second column). 40% of the NCN epidermal sections showed a strong positive expression of TDAG8. The other 60% exhibited a weak positive expression. TDAG8 occurrence in the NCN dermal part was similar to that in NCN epidermal portion (Figs. 3b,f,j, 5c and Supplementary Figs. S9–S12 second column). The BCC (Figs. 4b,f,j, 5b and Supplementary Figs. S13–S17 second column) showed a weak positive staining of TDAG8 in 33.3% of the cases and a negative staining in 66.7% of the samples.

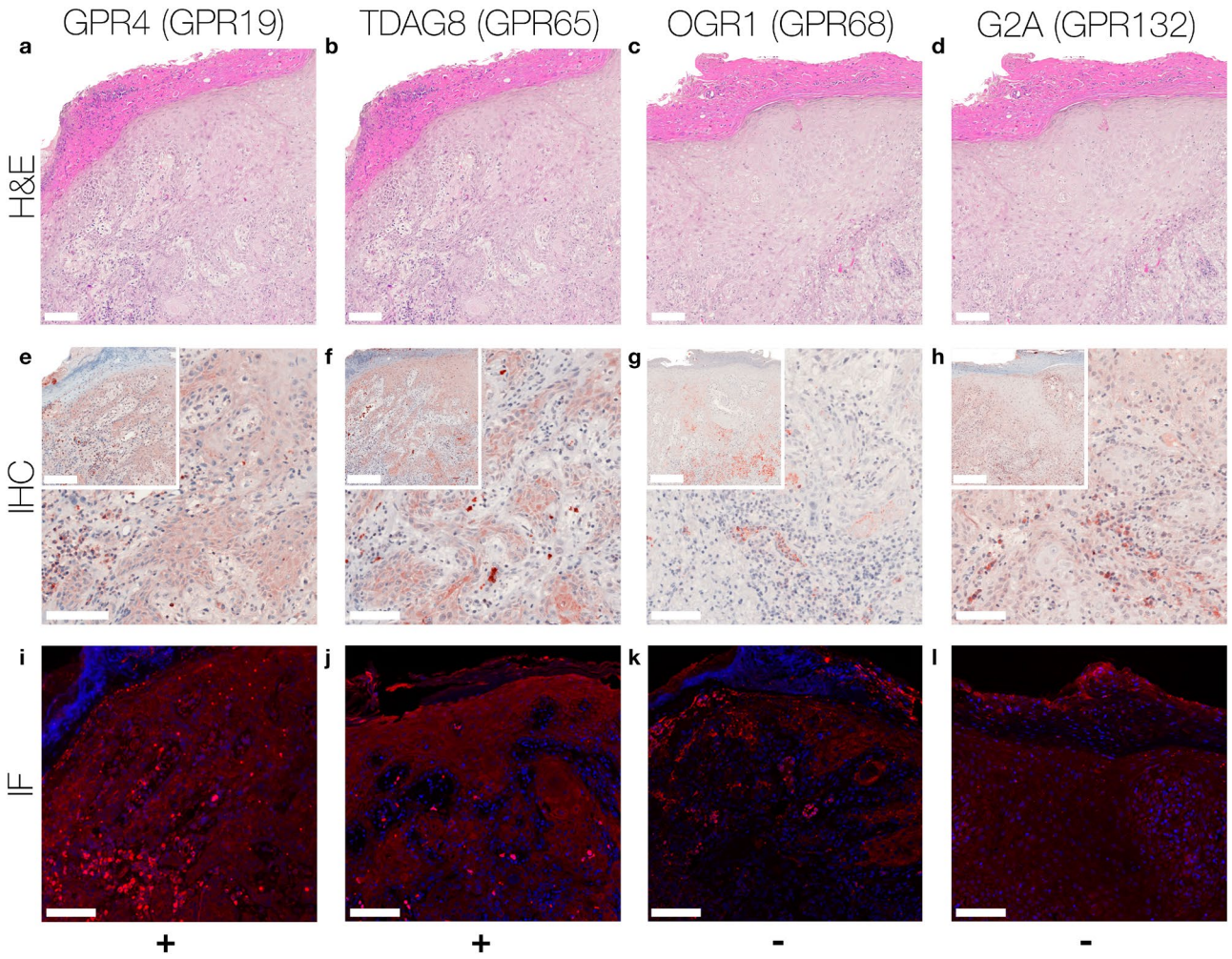

Figure 1. Immunohistochemistry and Immunofluorescence of SCC. Immunohistochemical and immunofluorescent staining for GPR4 (GPR19), TDAG8 (GPR65), OGR1 (GPR68) and G2A (GPR132) in SCC tissue. (**a**–**d**) histochemical H&E staining, (**e**–**h**) immunohistochemical staining, inserted images present a 2 × larger field of view, (**i**–**l**) immunofluorescence staining, red: secondary antibody label, blue: DAPI. Scale bars correspond to 100 µm (**a**–**l**: patient 1). Scores (bottom row) were assigned for ++: strong positive/positive reactions; +: weak positive/partial positive reaction; −: negative reaction. This SCC shows no expression of OGR1 and G2A in tumor cells, only several peritumoral lymphocytes appeared to be positive. The expression of GPR4 and TDAG8 is partial positive. For additional stainings of other SCC, see Figures S1–S4.

TMA. In the TMA, 87% of the SCC samples showed a weak positive expression, supporting the other immunostaining results (Fig. 6a, Fig. S18). The majority of MM strongly expressed TDAG8, where the epidermal section was strong positive in 78.3% and the dermal part in 69.6% (Fig. 6d). In contrast, NCN tumors appeared strong positive (57.9%) in their dermal section, while the epidermal portion was predominantly only weak positive (64.7%) (Fig. 6c). Large NCN tumor cells were strong positive for TDAG8 in both, dermal and epidermal tissue. 40.9% of the BCC cells were strong positive and 59.1% were either partial or weak positive (Fig. 6b).

Overall, the TMA corresponded well with the previous results, although the TMA did not show any negative results for TDAG8 in BCC.

OGR1 (GPR68). *IHC and IF.* The evaluation of the OGR1 (GPR68) expression-profiles based on IHC showed that 20% of SCC tissue samples were weak positive for OGR1, while the other 80% showed no expression of OGR1 (Figs. 1c,g,k, 5a, and Supplementary Figs. S1–S4 third column). 40% of MM epidermal tissue samples strongly expressed OGR1, 40% were weak positive and the other 20% were negative for OGR1. In contrast, 80% of the MM dermal sections showed a partial or weak positive expression and 20% showed no expression (Fig. 2c,g,k, 5d and Supplementary Figs. S5–S8 third column). 60% of the NCN epidermal tissue samples were weak positive and the other 40% strongly expressed OGR1. Dermal areas in NCN tissue samples revealed strong expression of OGR1 in 20% of the samples, partial expression in 60% of the cases and no expression in 20% of the tested samples (Figs. 3c,g,k, 5c and Supplementary Figs. S9–S12 third column). 33.3% of the BCC samples (Figs. 4c,g,k, 5b and Supplementary Figs. S13–S17 third column) were weak positive and the other 66.6% were negative for OGR1.

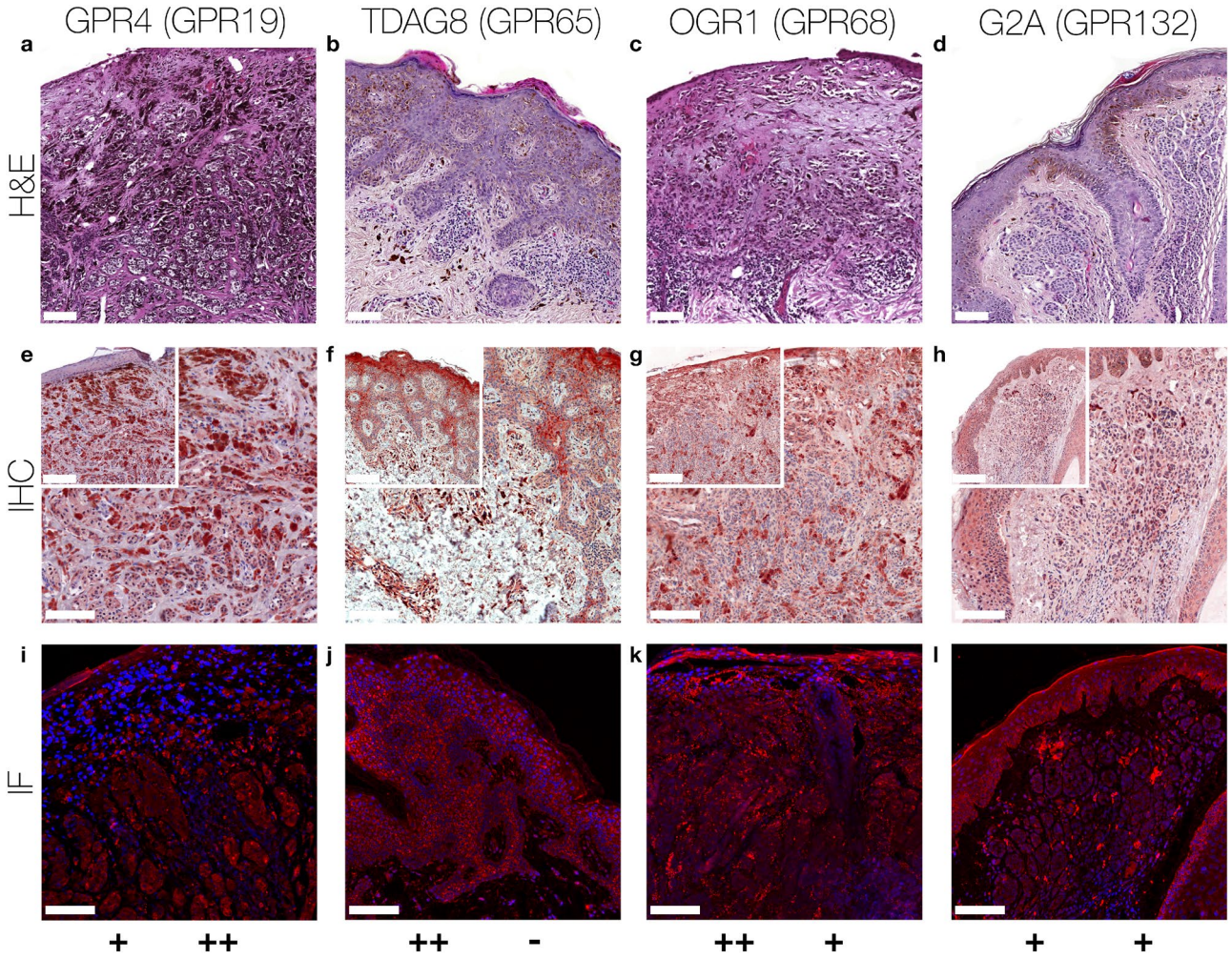

Figure 2. Immunohistochemistry and Immunofluorescence of MM. Immunohistochemical and immunofluorescent staining for GPR4 (GPR19), TDAG8 (GPR65), OGR1 (GPR68) and G2A (GPR132) in MM tissue. (**a**–**d**) histochemical H&E staining, (**e**–**h**) immunohistochemical staining, inserted images present a 2 × larger field of view, (**i**–**l**) immunofluorescence staining, red: secondary antibody label, blue: DAPI. Scale bars correspond to 100 µm (**a**,**c**,**e**,**g**,**i**,**k** patient 8; **b**,**d**,**f**,**h**,**j**,**l** patient 9). Scores (bottom row) were assigned for ++: strong positive/positive reactions; +: weak positive/partial positive reaction; −: negative reaction for the epidermal (left score) and the dermal (right score) portion. The MM shows a strong positive expression of TDAG8 and OGR1 in the epidermal portions. The epidermal expression of GPR4 and G2A is partial positive. There is a strong positive dermal expression of GPR4. OGR1 and G2A are weak positive regarding the dermal area and TDAG8 is not expressed dermally. Generally, smaller tumor cells within the tumor appear to be weakly positive, while below the epidermis multinuclear giant tumor cells with altered nucleus-cytoplasmic ratio are strongly expressed. For additional stainings of other MM, see Figures S5–S8.

TMA. 13% of the SCC cells were strong positive and 43.5% were weak positive, while 43.5% did not express OGR1 at all (Fig. 6a, Fig. S18). The epidermal part of MM was mostly positive for OGR1 (95.5%), whereas the MM dermal section appeared predominantly weak positive (63.6%) (Fig. 6d). Dermal MM cells appear to be partially strong positive. 64.3% of the NCN epidermal portion was OGR1 negative, while the NCN dermal part reached 100% weak positive results (Fig. 6c). About 75% of the BCC cells expressed OGR1 positive, while 25% did not express this GPCR (Fig. 6b).

Taken together, the TMA correlated with the results of the IHC/IF except of the BCC. According to the TMA data, BCC were more likely positive for OGR1.

G2A (GPR132). *IHC and IF.* 40% of the SCC tissue samples presented a clearly positive expression of G2A (GPR132), 40% appeared to be weak or partial positive and the other 20% showed no expression of G2A (Figs. 1d,h,l, 5a and Supplementary Figs. S1–S4 fourth column). In 20% of the samples, the MM epidermal sections showed a strong, in 60% a weak positive expression of G2A and in 20% of the cases there was no expression of G2A. In dermal areas of MM 20% of the MM samples strongly expressed G2A, while 80% showed a weak positive expression (Figs. 2d,h,l, 5d and Supplementary Figs. S5–S8 fourth column). Both NCN epidermal and dermal parts provided either strong or partial weak positive results: 40% of NCN samples were strong positive

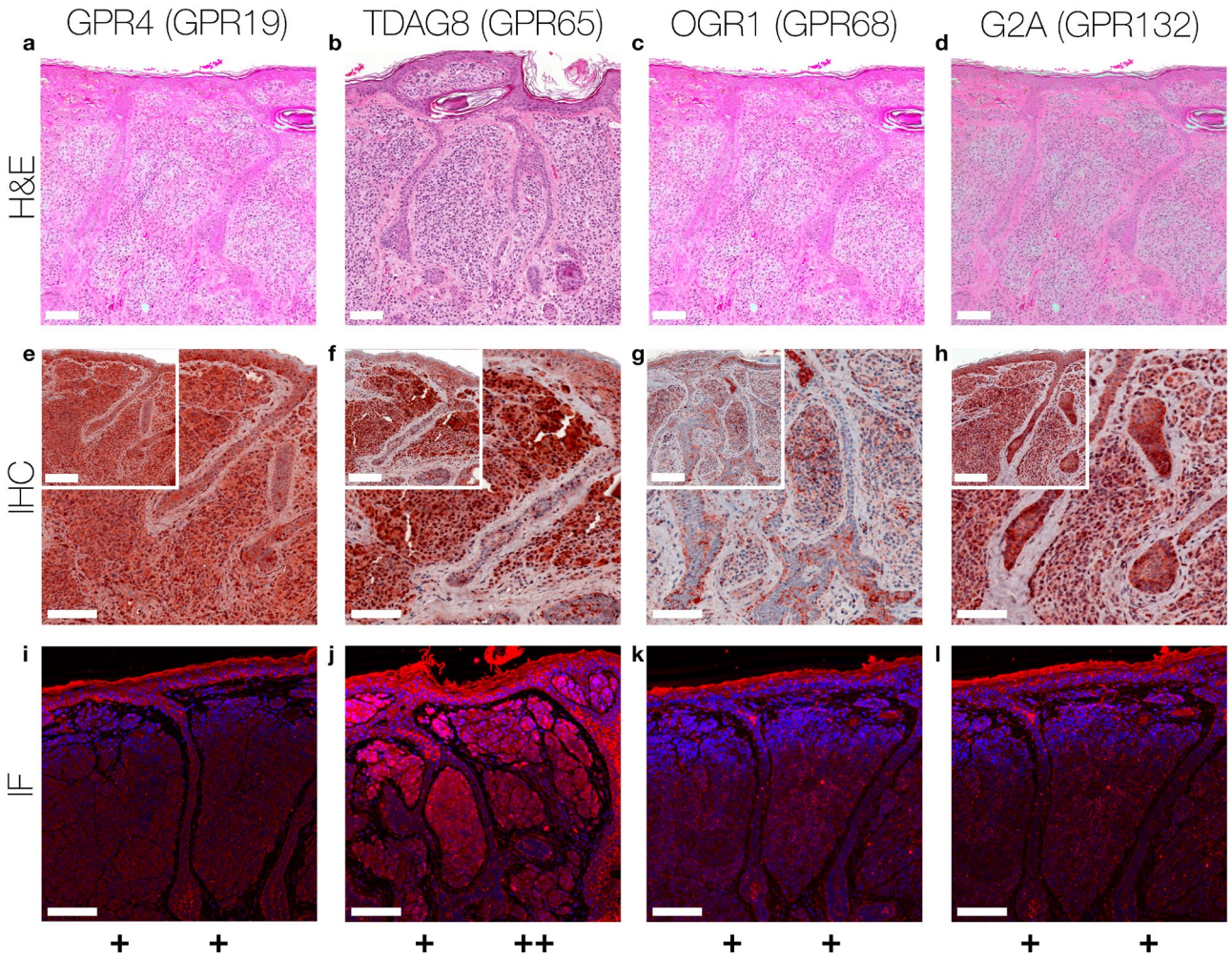

Figure 3. Immunohistochemistry and Immunofluorescence of NCN. Immunohistochemical and immunofluorescent staining for GPR4 (GPR19), TDAG8 (GPR65), OGR1 (GPR68) and G2A (GPR132) in NCN tissue. (**a**–**d**) histochemical H&E staining, (**e**–**h**) immunohistochemical staining, inserted images present a 2 × larger field of view, (**i**–**l**) immunofluorescence staining, red: secondary antibody label, blue: DAPI. Scale bars correspond to 100 µm (**a**–**l** patient 15). Scores (bottom row) were assigned for ++: strong positive/positive reactions; +: weak positive/partial positive reaction; −: negative reaction for the epidermal (left score) and the dermal (right score) portion. The NCN shows a partial positive expression of all GPCRs on the epidermal portions. There are even some epidermal tumor cells strongly expressed in the TDAG8. Regarding the dermal area GPR4, OGR1 and G2A are weak positive, while MM shows a significantly increased expression of TDAG8. For additional stainings of other NCN, see Figures S9–S12.

and 60% were weak positive for cells within the epidermal portion of NCN. In the case of the NCN dermal section the results were inverse: 60% showed strong positive expression of G2A, but only 40% were weak positive (Figs. 3d,h,l, 5c and Supplementary Figs. S9–S12 fourth column). Regarding the expression of G2A on BCC cells (Figs. 4d,h,l, 5b and Supplementary Figs. S13–S17 fourth column), about 50% of the tissue samples strongly expressed G2A and 50% of the specimen were partial positive.

TMA. 83.4% of the SCC cells showed a weak G2A expression, 8.3% of the samples revealed strong positive expression and the other 8.3% were negative for G2A (Fig. 6a, Fig. S18). 52.4% of the MM epidermal section expressed G2A strongly and 85.7% of the dermal portion of MM had a weak positive expression (Fig. 6d). Giant MM tumor cells appeared to be strong positive in the epidermal and dermal parts. The NCN dermal part appeared to be mostly weak positive (88.2%) in contrast to the NCN epidermal zone, which revealed more negative results (33.3%) (Fig. 6c). 60% of the BCC cells expressed G2A weakly, whereas 40% of BCC showed strong expression (Fig. 6b). The TMA results fully confirmed the IHC/IF results.

Discussion

In this study, we have examined the expression profiles of the pH-GPCRs GPR4 (GPR19), TDAG8 (GPR65), OGR1 (GPR68) and G2A (GPR132) on different types of common skin tumors, SCC, MM, NCN and BCC. Each tumor expresses typical sets of GPCRs: (1) GPR4 is expressed on all epidermal portions of NCN (IHC: 40%

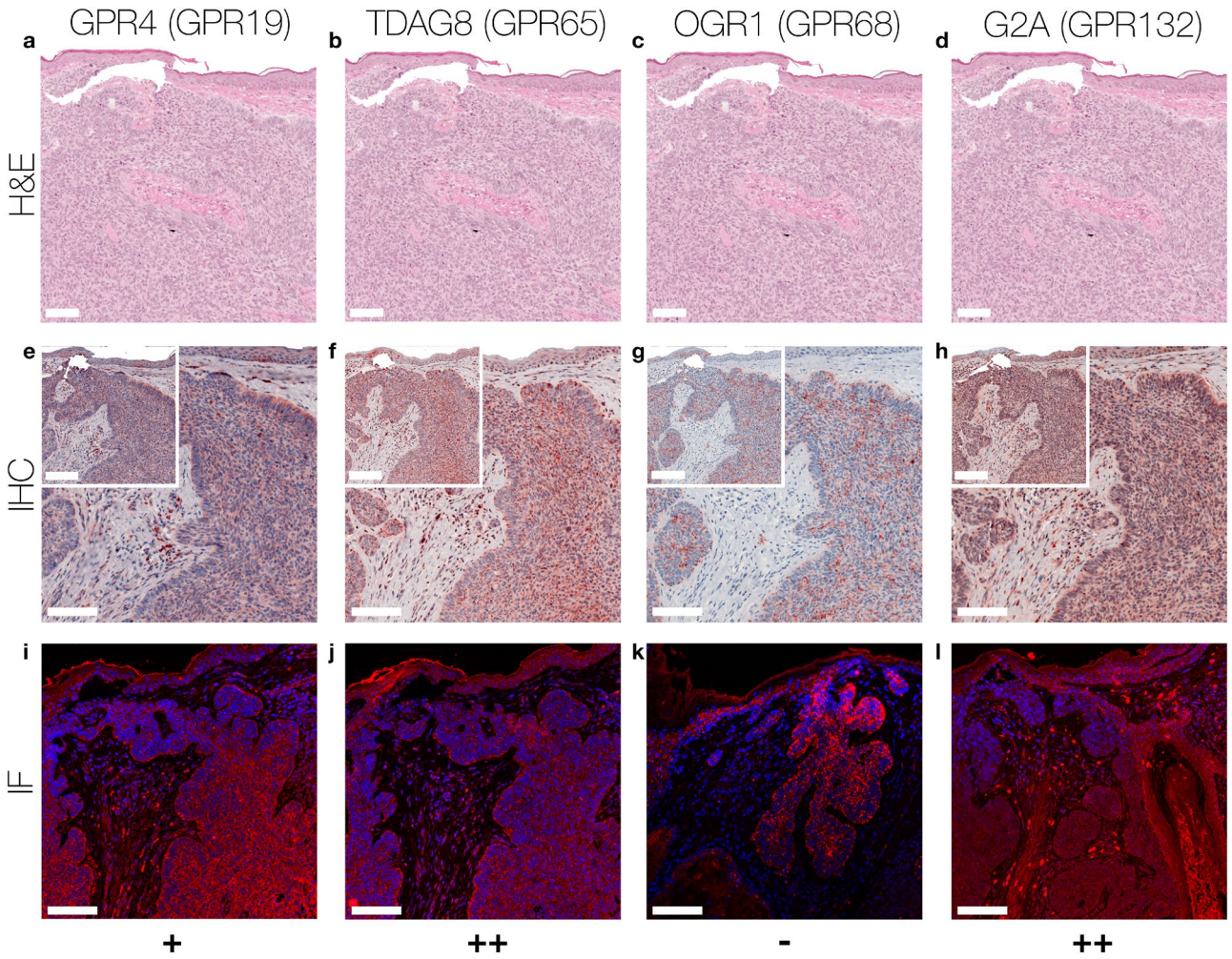

Figure 4. Immunohistochemistry and Immunofluorescence of BCC. Immunohistochemical and immunofluorescent staining for GPR4 (GPR19), TDAG8 (GPR65), OGR1 (GPR68) and G2A (GPR132) in BCC tissue. (**a**–**d**) histochemical H&E staining, (**e**–**h**) immunohistochemical staining, inserted images present a 2 × larger field of view, (**i**–**l**) immunofluorescence staining, red: secondary antibody label, blue: DAPI. Scale bars correspond to 100 µm (**a**–**l** patient 20). Scores (bottom row) were assigned for ++: strong positive/positive reactions; +: weak positive/partial positive reaction; −: negative reaction. The expression of TDAG8 and G2A on the surface of BCC tumor cells is significantly increased, while the expression of GPR4 is weakly positive. No expression of OGR1 is detected. For additional stainings of other BCC, see Figures S13–S17.

++, 60% +, TMA: 38.9% ++, 61,1% +) and on epidermal (IHC: 20% ++, 40% +, TMA: 94.7% ++, 5.3% +) and dermal (IHC: 60% ++, 40% +, TMA: 52.6% ++, 15.8% +) MM. (2) G2A is clearly expressed on BCC (IHC: 50% ++, 50% +, TMA: 40% ++, 60% +) and the dermal MM area (IHC: 20% ++, 80% +, TMA: 14.3% ++, 85,7% +), while expression is also seen for epidermal MM portions (IHC: 20% ++, 40% +, TMA: 52.4% ++, 47.6% +) and NCN (mostly dermal). (3) TDAG8 is expressed on SCC (IHC: 20% ++, 80% +, TMA: 13% ++, 87% +), strongly on the epidermal MM (IHC: 60% ++, 40% +, TMA: 78,3% ++, 12.7% +) as well as the dermal portions of NCN (IHC: 40% ++, 60% +, TMA: 57,9% ++, 42.1% +) and (4) OGR1 is poorly expressed on SCC (IHC: 80%−, TMA: 43,5%−). It is striking, that all four GPCRs are particularly often expressed in NCN and MM. Mixed results were found for any other combination of pH-GPCR and tumor type (Figs. 5 and 6).

The very inhomogeneous expression-profiles support the current knowledge about the opposing roles of the four pH-GPCRs within a tumor[14]. The pH-GPCRs function as proton signal sensors and transducers[12] and consequently, have an effect on cancer cell proliferation, metastasis, angiogenesis, apoptosis, immune cell function and inflammation, either in a pro-tumorigenic or in an anti-tumorigenic manner[12,23–25,27–29]. The role of the individual pH-GPCRs in tumor progression/regression and the impact of either overexpression or depletion of individual pH-GPCR types on different cell types is yet to be investigated.

GPR4 (GPR19). GPR4 is expressed on all epidermal NCN portions. Dermal NCN, MM, SCC and BCC varied in expression levels. While dermal NCN portions, SCC and BCC exhibited weak positive results, dermal MM showed strong positive results. Interestingly, the TMA stated a strong positive expression of GPR4 in the epidermal MM, and IHC/IF predominantly showed (strong) positive results for the epidermal portion of MM

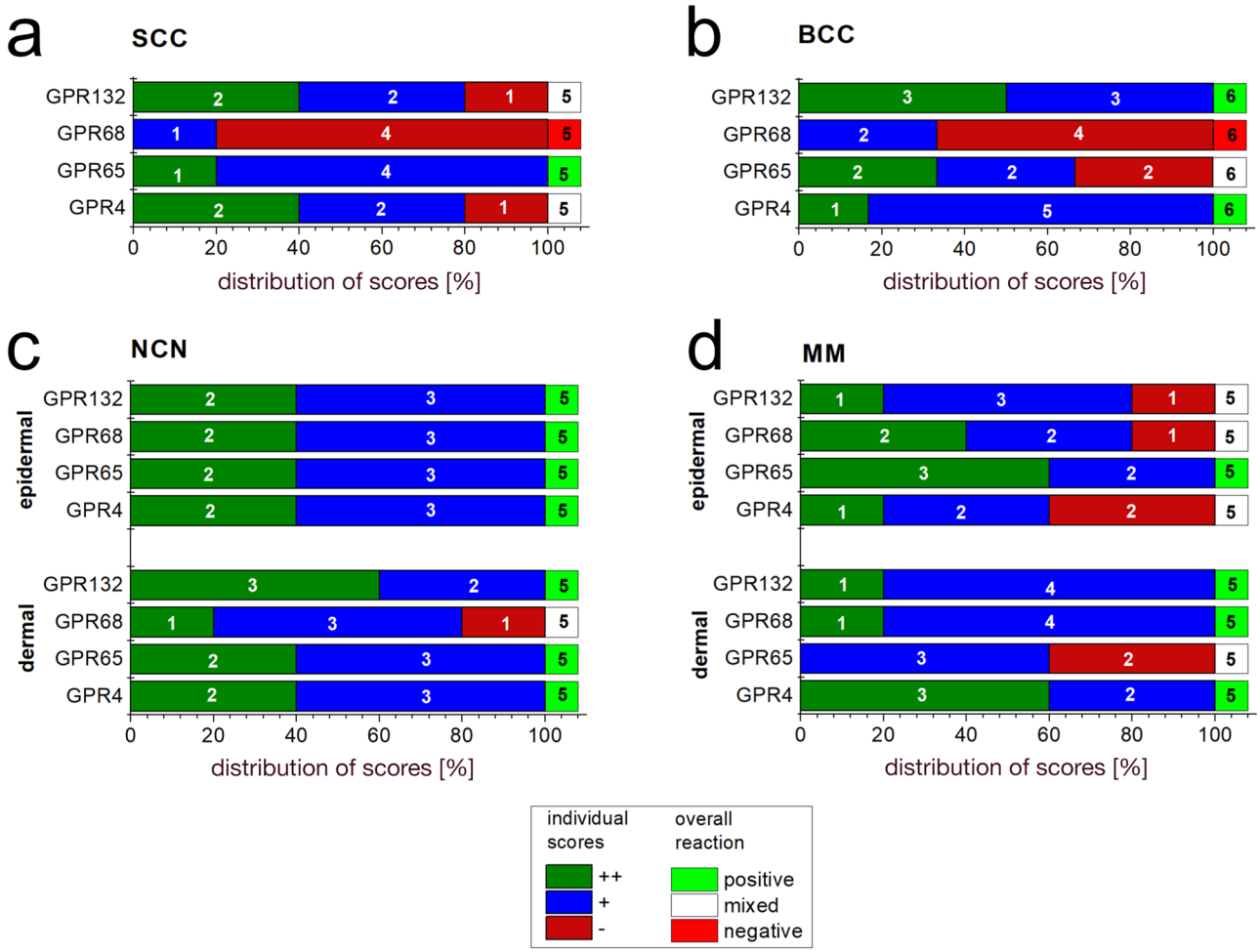

Figure 5. IHC-Score results for different pH-GPCRs in common skin tumors. Fractional distribution of the scores (green bar, ++: strong positive/positive reaction; +, blue bar: weak positive/ partial positive reaction; −, red bar: negative reaction) for GPR4 (GPR19), TDAG (GPR65), OGR1 (GPR68) and G2A (GPR132) of immunohistochemically stained skin tumors (**a**) SCC, (**b**) BCC, (**c**) NCN, (**d**) MM. MM and NCN are further subclassified in epidermal and dermal portions. Numbers in bars indicate the occurrence of a respective score. The sum of all scores is 100%. Overall evaluation is indicated by a green, white or red box (beyond 100% scale): green box: overall positive reactions; red box: overall negative reactions; white box: mixed reactions without clear majority in favour of one specific reaction. Numbers in this box indicate the total number of samples investigated.

except of two tissue samples. GPR4 was found to be overexpressed in several human cancers[31]. GPR4-deficient mice showed a significantly reduced angiogenic response to VEGF, which accordingly led to a reduction in tumor growth in orthotopic models[29]. Acidification-activated GPR4 in endothelial cells increased the expression of a number of inflammatory genes and promoted angiogenesis in head and neck cancer, likely via secretion of angiogenic factors[32]. Regarding cancer cells themselves, it was shown that ectopic expression of GPR4 in murine 3T3 cells induced malignant transformation[33]. In contrast, GPR4 overexpression in B16F10 melanoma cells inhibited their acidic pH-induced migration, invasion and metastasis formation[22]. Taking this knowledge and our results into account, GPR4 might be an indicator of dysplasia of dermal melanocytes similar to HMB45. The latter is also found to often remain positive in deep dermal portions of dysplastic nevi or melanoma while expression levels decrease with increasing depth in normal nevi.

TDAG8 (GPR65). In all four tumor types investigated in this study expression of TDAG8 was high, except for dermal portions of MM, epidermal portions of NCN and BCC, where TDAG8 occurrence was often only moderate or missing. TDAG8 is predominantly expressed in lymphoid cells and tissues, including peripheral blood leukocytes, spleen, lymph nodes, and thymus and has also been detected in some selected cancers[31,34]. Overexpression of TDAG8 in lung carcinoma cells was associated with enhanced tumor development and cancer cell survival under acidic conditions[33]. Ectopic TDAG8 expression malignantly transformed a normal mammary epithelial cell line and led to ligand-independent activation of SRE and CRE promoter-driven gene transcription in HEK293 cells[31]. On the other hand, ectopic overexpression of TDAG8-GFP fusion protein enhanced apoptosis and sensitivity to dexamethasone-induced apoptosis in lymphoma cells[35]. TDAG8-deficiency in different KO

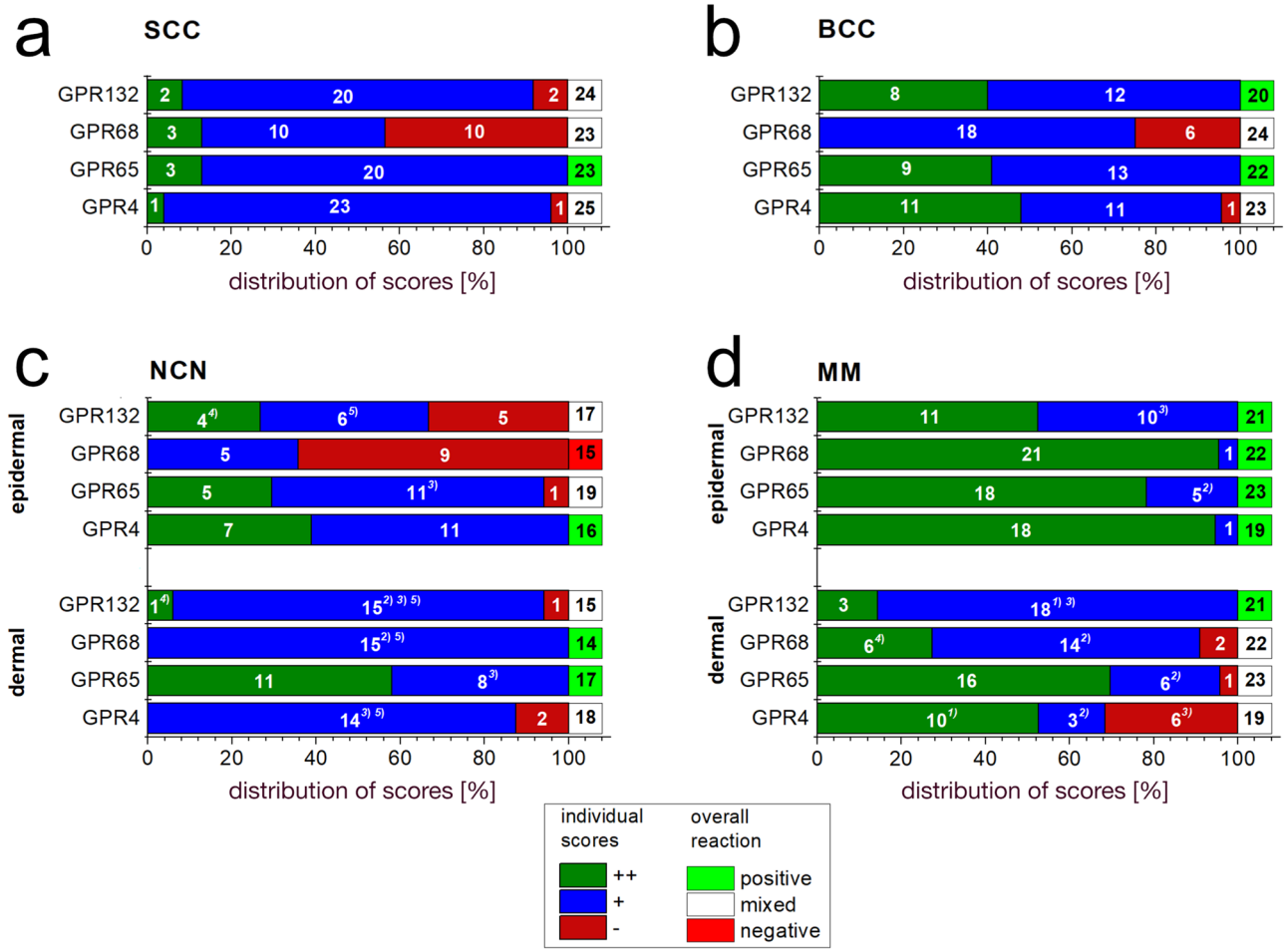

Figure 6. TMA-Score results for different pH-GPCRs in common skin tumors. Fractional distribution of the scores (green bar, ++: strong positive/positive reaction; +, blue bar: weak positive/ partial positive reaction; –, red bar: negative reaction) for GPR4 (GPR19), TDAG (GPR65), OGR1 (GPR68) and G2A (GPR132) of TMAs on different skin tumors (**a**) SCC, (**b**) BCC, (**c**) NCN, (**d**) MM. MM and NCN are further subclassified in epidermal and dermal portions. Numbers in bars indicate the occurrence of a respective score. The sum of all scores is 100%. Superscript numbers give information on scoring details: (1) strong positive either on the surface or in the deeper parts of the tumor tissue, (2) single tumor cells are strong positive, but the overall impression is weak positive, (3) large tumor cells appear strong positive, (4) partially strong positive and (5) weak positive. Overall evaluation is indicated by a green, white or red box (beyond 100% scale): green box: overall positive reactions; red box: overall negative reactions; white box: mixed reactions without clear majority in favour of one specific reaction. Numbers in this box indicate the total number of samples investigated. For additional information on the individual TMA score, see Supplementary Tables S2–S5.

mouse models was associated with an exacerbation of inflammation in selected pathologies[36–38]. In summary, it seems that TDAG8 attenuates immune-mediated inflammation, while the overall effect on non-blood-cell tumor cell behaviour remains less clear. Based on this knowledge, we hypothesize that the high expression of TDAG8 in the investigated skin tumors might be crucial for tumor growth and/or tumor cell survival. However, another possible mechanism could be that TDAG8 acts as a tumor suppressive receptor to control tumor growth under acidic conditions. These questions have to be addressed with cell culture experiments.

OGR1 (GPR68). Regarding the tumor tissue analysed in this study, OGR1 is not (IHC) or only moderately (TMA) expressed in SCC and BCC, but particularly present in MM and NCN. Overexpression of OGR1 in human prostate and ovarian cancer cells mediated an inhibitory effect on cell migration and metastasis[27,28,39]. In addition, OGR1 overexpression in ovarian cancer cells also inhibited cell proliferation, while increasing cell–matrix adhesion[27], suggesting a tumor-supressing effect of ORG1. In contrast, when the host cells of ORG1 knock-out mice were depleted of ORG1 the tumorigenesis of injected melanoma cells and prostate cancer cells was decreased[40,41], indicating tumor-promoting function of ORG1 in the host organism. In other cell types ORG1 expression and acid stimulation was associated with the expression of inflammatory and immune modulatory factors[42–45]. These findings state that the high expression of ORG1 in the mesenchymal tumors NCN and

MM clearly differs from the expression in the epithelial tumors SCC and BCC. Further cell culture experiments are needed in order to study the exact effect of OGR1 in the skin.

G2A (GPR132). In skin G2A (GPR132) is proposedly expressed in keratinocytes, fibroblasts, epidermal cells and melanocytes[14]. The incidence of G2A in the investigated tumors was high in both, epidermal and dermal parts of MM, NCN and BCC, but less frequent in SCC. G2A is predominantly expressed by different immune cells[46,47]. G2A was identified as a stress-inducible gene, activated by genetic recombination processes in immature B lymphocytes and developing thymocytes, or by exposure to DNA-damaging stress, like UV, X-ray, etoposide or doxorubicin[48]. G2A expression led to cell cycle arrest and attenuated transformation potential of oncogenes[48]. The important role of G2A in controlling immune cell homeostasis was supported by the finding that G2A-deficiency caused autoimmune syndrome in ageing G2A-depleted mice[49]. However, expression of G2A in other cell types appears to have oncogenic potential, as high-level expression of G2A in NIH3T3 cells induced malignant transformation[50]. In human epidermal keratinocytes, G2A mediated the secretion of cytokines, and induced cell cycle arrest[46]. UVB radiation and H_2O_2 enhanced G2A expression in HaCaT cells, indicating that G2A might function as sensor for DNA damage and oxidative stress in keratinocytes[51]. With its high expression in skin tumors MM, NCN, SCC and BCC, G2A might play a pivotal role as an immune checkpoint of the tumor.

Regarding the expression of pH-GPCRs in different skin tumors, TMA results (Fig. 6) reveal that the overall expression of all four GPCRs increases in MM compared to NCN. Especially the incidence of strong positive expression of the pH-GPCRs is increased in both, dermal and, even more pronounced, in epidermal portions. Thus results suggest that an increase in pH-GPCR expression in MM could be a marker for increased malignancy, which requires, however, further investigation.

The prevailing hypothesis, that influencing factors such as type of cancer, the micro- and macro environment as well as the variation between every human individual influence individual pH-GPCR expression, can be supported with the results of this study, containing a large data set for the four most common skin cancers.

In summary, the current evidence on the expression of pH-GPCRs in tumors is still only a first step towards understanding the role of pH-GPCRs and their function as transmembrane messengers of extracellular pH in cancer development or control. Further functional studies are undoubtedly required to fully understand the individual role of each pH-GPCR in the development and progression of different skin cancers.

The cancer type-specific differential expression of individual pH-GPCRs underpins their potential value in the field of cancer therapy. Our investigations may lead to more specific cell culture studies of the pH-GPCRs in different skin tumor cell lines and their use as a potential therapeutic target.

Materials and methods

Tissue samples. For all experiments, we used tissue samples older than 10 years from the department of Dermatology at the University Medical Center Regensburg (IHC/IF: n = 5, exception: BCC n = 6; TMA: n = 24–27). Routine paraffin-embedded skin biopsies obtained from affected areas of patients with localized skin tumors were used anonymized. The diagnosis of localized tumors had been previously confirmed histologically by a dermatopathologist. Handling of human skin tumor biopsies older than 10 years was approved by the ethical committee of the University of Regensburg. Under German law the tumor tissue left after surgery after the final diagnosis can be discarded after 10 years or are free to use.

General data regarding the tissue sample origin is given in Supplementary Table S1. The following tissue types served as positive controls: primary human tonsil tissue and lung tissue for G2A and TDAG8, endosomal membrane of the testis and lung for OGR1 and pancreas as well as the endosomal membrane of the lung for GPR4. As negative control tissue we used liver for GPR4, heart muscle for GPR65, pancreas for GPR68 and ovary for GPR132. Respective images from IHC staining on control tissue including secondary antibody controls and isotype antibody controls are shown in supplementary figure S19. Additional antibody controls on dermal tumor tissue are shown in supplementary figure S20.

Immunohistochemistry (IHC). Hematoxylin and eosin (HE)-stained, paraffin-embedded and fixed tissues as well as positive and negative controls were freshly cut into 2 µm thin pieces and superimposed on slides. Tissue sections were incubated for 30 min at 72 °C before they were rehydrated by washing with alcohol solutions at descending concentrations as follows: 2 × xylol for 5 min, 2 × 100% ethanol for 5 min, 2 × 96% Ethanol for 5 min, 2 × 70% ethanol for 5 min. Endogenous peroxidase was neutralised by incubation with 3% H_2O_2 (Fisher Scientific GmbH, Schwerte, Germany) for 10 min. Afterwards, the slides were washed in distilled water and were submersed in precooked citrate buffer (boiled for 30 min) (Zytomed Systems GmbH, Berlin, Germany) for 20 min. After cooling the sections on ice, they were incubated in phosphate-buffered saline (PBS) (Sigma-Aldrich, St. Louis, United States of America) for 10 min at RT. Subsequently, sections were clamped to Shandon coverplate immunostaining chambers Fisher Scientific GmbH, Schwerte, Germany) and transferred to PBS. Samples were incubated for 10 min at RT in a blocking solution (ZytoChem Plus HRP Kit/Rabbit, Zytomed Systems GmbH, Berlin, Germany) in order to minimise unspecific binding of antibodies.

In the following, tissue sections were treated with polyclonal primary antibody (rabbit anti-human GPR4 (1:200; Abcam, Cambridge, Great Britain, Anti-GPCR GPR4 antibody, ab188606), GPR65 (1:500; Abcam, Cambridge, Great Britain, Anti-GPCR GPR65 antibody, ab188907), GPR68 (1:50; Abcam, Cambridge, Great Britain, Anti-OGR1 antibody, ab188964) and GPR 132 (1:60; Abcam, Cambridge, Great Britain, Anti-GPCR G2A antibody, ab116586) or isotype control antibody (1:200, Abcam, Cambridge, Great Britain, rabbit IgG polyclonal isotype control, ab27478) in antibody diluent (Zytomed Systems GmbH, Berlin, Germany) overnight at 4 °C. The following day, sections were rinsed in PBS (3 × 5 min) and then incubated with the secondary biotinylated antibody (ZytoChem Plus HRP Kit/Rabbit, Zytomed Systems GmbH, Berlin, Germany) for 30 min at RT. After

three washes with PBS, samples were incubated with streptavidin-HRP-conjugate for 20 min at RT, followed by another washing step with PBS. Finally, chromogen solution AEC plus (Dako, Glostrup, Denmark), was added. The reaction was stopped by several washes with distilled water as soon as the positive controls showed distinct staining. Mayer's Haemalm (Carl Roth GmbH & Co., Karlsruhe, Germany) was used to counterstain the tissue. Samples were embedded with Aquetex mounting medium (Merck KGaA, Darmstadt, Germany).

Specimen were inspected with a Leitz Wild Biomed microscope (Leica Microsystems GmbH, Wetzlar, Germany, Type: 020-507.010) and afterwards scanned with the PreciPoint M8. Digital images were edited using the analysis software ViewPoint online (PreciPoint, Freising, Germany). Images were evaluated via visual inspection. Scores were assigned for ++: strong positive/positive reaction; +: weak positive/partial positive reaction; −: negative reaction.

Tissue microarray (TMA). The immunohistochemical multiple-labelling tissue microarray (TMA) allows for simultaneous IHC staining of multiple tissue samples. Representative tumor material from 24–27 tissue samples per tumor type was assembled into a paraffin matrix (5 × 6) with 1 mm diameter spots. Samples on the TMA tissue slide were subjected to IHC staining following the protocol above.

Immunofluorescence (IF). Samples were incubated in the heating cabinet for 20 min at 70 °C and rehydrated with the descending order of the alcohol concentration as described above. The slides were washed with PBS and subsequently incubated in citrate-tris-EDTA-buffer (Zytomed Systems GmbH, Berlin, Germany) for 25 min. The sections were cooled on ice for 25 min and then submersed in PBS for 10 min. The samples were incubated for 15 min in tris-glycine-buffer (Trishydroxymethylaminomethan: Merck KGaA, Darmstadt, Germany; Glycine: Merck KGaA, Darmstadt, Germany) to reduce autofluorescence. After three rinses with PBS, samples were incubated with 5% BSA (Sigma-Aldrich, St. Louis, United States of America) in tris-buffered saline with 0.1% Tween-20 (TBST) (Tween-20: Carl Roth GmbH & Co., Karlsruhe, Germany) for 60 min in order to block unspecific binding of antibodies. Tissue sections were incubated with primary antibody (GPR4 1:100, GPR65 1:300; GPR68 1:250, GPR132 1:60) in phosphate-buffered saline 1% Tween-20 (PBST) at 4 °C overnight. Afterwards, samples were washed three times for 15 min. Alexa-594-conjugated goat anti-rabbit specific second antibody (Life Technologies, Carlsbad, United States of America, A11037) was diluted with 1% BSA in PBST (1:1,000) and added to the slides for 30 min. Afterwards, tissue sections were rinsed once with PBS for 15 min, and finally stained for cell nuclei with 4,5-diamindino-2-phenylindole (DAPI). Fluorescence was exposed with a Zeiss Axio Imager.

Scoring. Scoring was based on visual assessment of cell number and intensity of staining. The grades were: ++: strong positive/positive histochemical reaction, with > 80% of cells positive and/or high staining intensity; +: weak positive/ partial positive reaction, with 20—80% of cells positive and staining weak or only partially strong; −: negative reaction, with < 20% cells with weak staining. Assessment was done by two experienced histopathologists. Further comments were made if necessary: (1) strong positive either on the surface or in the deeper parts of the tumor tissue, (2) single tumor cells are strong positive, but the overall impression is weak positive, (3) large tumor cells appear strong positive, (4) partially strong positive and (5) weak positive.

Ethics. All experiments were done in accordance with the declaration of Helsinki. No identifying data of tissue donors were used during experiments or in the paper. All tissue samples were from patients older than 18 years.

Received: 16 July 2020; Accepted: 19 August 2020

References

1. Siegel, R. L., Miller, K. D. & Jemal, A. Cancer statistics, 2019. *CA Cancer J. Clin.* **69**, 7–34. https://doi.org/10.3322/caac.21551 (2019).
2. Apalla, Z., Nashan, D., Weller, R. B. & Castellsague, X. Skin cancer: Epidemiology, disease burden, pathophysiology, diagnosis, and therapeutic approaches. *Dermatol. Ther. (Heidelb)* **7**, 5–19. https://doi.org/10.1007/s13555-016-0165-y (2017).
3. Augustin, J., Kis, A., Sorbe, C., Schafer, I. & Augustin, M. Epidemiology of skin cancer in the German population: Impact of socioeconomic and geographic factors. *J. Eur. Acad. Dermatol. Venereol.* **32**, 1906–1913. https://doi.org/10.1111/jdv.14990 (2018).
4. Hanlon, A. Metastatic squamous cell carcinoma: epidemiology and available systemic therapies. *Curr. Dermatol. Rep.* **2**, 118–124. https://doi.org/10.1007/s13671-013-0047-9 (2013).
5. Mackiewicz-Wysocka, M., Bowszyc-Dmochowska, M., Strzelecka-Weklar, D., Danczak-Pazdrowska, A. & Adamski, Z. Basal cell carcinoma—Diagnosis. *Contemp. Oncol. (Pozn)* **17**, 337–342. https://doi.org/10.5114/wo.2013.35684 (2013).
6. Viana, A. C., Gontijo, B. & Bittencourt, F. V. Giant congenital melanocytic nevus. *An. Bras. Dermatol.* **88**, 863–878. https://doi.org/10.1590/abd1806-4841.20132233 (2013).
7. Damsky, W. E. & Bosenberg, M. Melanocytic nevi and melanoma: Unraveling a complex relationship. *Oncogene* **36**, 5771–5792. https://doi.org/10.1038/onc.2017.189 (2017).
8. Linares, M. A., Zakaria, A. & Nizran, P. Skin Cancer. *Prim. Care* **42**, 645–659. https://doi.org/10.1016/j.pop.2015.07.006 (2015).
9. Zbytek, B. *et al.* Current concepts of metastasis in melanoma. *Expert Rev. Dermatol.* **3**, 569–585. https://doi.org/10.1586/17469872.3.5.569 (2008).
10. Graul, R. C. & Sadee, W. Evolutionary relationships among G protein-coupled receptors using a clustered database approach. *AAPS Pharm. Sci.* **3**, E12. https://doi.org/10.1208/ps030212 (2001).

11. Lee, H. J., Wall, B. & Chen, S. G-protein-coupled receptors and melanoma. *Pigment Cell Melanoma Res.* **21**, 415–428. https://doi.org/10.1111/j.1755-148X.2008.00478.x (2008).
12. Ludwig, M. G. *et al.* Proton-sensing G-protein-coupled receptors. *Nature* **425**, 93–98. https://doi.org/10.1038/nature01905 (2003).
13. Justus, C. R., Dong, L. & Yang, L. V. Acidic tumor microenvironment and pH-sensing G protein-coupled receptors. *Front. Physiol.* **4**, 354. https://doi.org/10.3389/fphys.2013.00354 (2013).
14. Weiss, K. T. *et al.* Proton-sensing G protein-coupled receptors as regulators of cell proliferation and migration during tumor growth and wound healing. *Exp. Dermatol.* **26**, 127–132. https://doi.org/10.1111/exd.13209 (2017).
15. Nassios, A. *et al.* Expression of proton-sensing G-protein-coupled receptors in selected skin tumors. *Exp. Dermatol.* **28**, 66–71. https://doi.org/10.1111/exd.13809 (2019).
16. Im, D. S. Orphan G protein-coupled receptors and beyond. *Jpn. J. Pharmacol.* **90**, 101–106. https://doi.org/10.1254/jjp.90.101 (2002).
17. Cardone, R. A., Casavola, V. & Reshkin, S. J. The role of disturbed pH dynamics and the Na+/H+ exchanger in metastasis. *Nat. Rev. Cancer* **5**, 786–795. https://doi.org/10.1038/nrc1713 (2005).
18. Webb, B. A., Chimenti, M., Jacobson, M. P. & Barber, D. L. Dysregulated pH: A perfect storm for cancer progression. *Nat. Rev. Cancer* **11**, 671–677. https://doi.org/10.1038/nrc3110 (2011).
19. Neri, D. & Supuran, C. T. Interfering with pH regulation in tumours as a therapeutic strategy. *Nat. Rev. Drug Discov.* **10**, 767–777. https://doi.org/10.1038/nrd3554 (2011).
20. Tomura, H., Mogi, C., Sato, K. & Okajima, F. Proton-sensing and lysolipid-sensitive G-protein-coupled receptors: A novel type of multi-functional receptors. *Cell Signal.* **17**, 1466–1476. https://doi.org/10.1016/j.cellsig.2005.06.002 (2005).
21. Haverkampf, S. *et al.* NHE1 expression at wound margins increases time-dependently during physiological healing. *Exp. Dermatol.* **26**, 124–126. https://doi.org/10.1111/exd.13097 (2017).
22. Castellone, R. D., Leffler, N. R., Dong, L. & Yang, L. V. Inhibition of tumor cell migration and metastasis by the proton-sensing GPR4 receptor. *Cancer Lett.* **312**, 197–208. https://doi.org/10.1016/j.canlet.2011.08.013 (2011).
23. Chen, A. *et al.* Activation of GPR4 by acidosis increases endothelial cell adhesion through the cAMP/Epac pathway. *PLoS ONE* **6**, e27586. https://doi.org/10.1371/journal.pone.0027586 (2011).
24. Dong, L. *et al.* Acidosis activation of the proton-sensing GPR4 receptor stimulates vascular endothelial cell inflammatory responses revealed by transcriptome analysis. *PLoS ONE* **8**, e61991. https://doi.org/10.1371/journal.pone.0061991 (2013).
25. He, X. D. *et al.* Involvement of proton-sensing receptor TDAG8 in the anti-inflammatory actions of dexamethasone in peritoneal macrophages. *Biochem. Biophys. Res. Commun.* **415**, 627–631. https://doi.org/10.1016/j.bbrc.2011.10.122 (2011).
26. Mogi, C. *et al.* Involvement of proton-sensing TDAG8 in extracellular acidification-induced inhibition of proinflammatory cytokine production in peritoneal macrophages. *J. Immunol.* **182**, 3243–3251. https://doi.org/10.4049/jimmunol.0803466 (2009).
27. Ren, J. & Zhang, L. Effects of ovarian cancer G protein coupled receptor 1 on the proliferation, migration, and adhesion of human ovarian cancer cells. *Chin. Med. J. (Engl.)* **124**, 1327–1332 (2011).
28. Singh, L. S. *et al.* Ovarian cancer G protein-coupled receptor 1, a new metastasis suppressor gene in prostate cancer. *J. Natl. Cancer Inst.* **99**, 1313–1327. https://doi.org/10.1093/jnci/djm107 (2007).
29. Wyder, L. *et al.* Reduced pathological angiogenesis and tumor growth in mice lacking GPR4, a proton sensing receptor. *Angiogenesis* **14**, 533–544. https://doi.org/10.1007/s10456-011-9238-9 (2011).
30. Yang, L. V. *et al.* Vascular abnormalities in mice deficient for the G protein-coupled receptor GPR4 that functions as a pH sensor. *Mol. Cell. Biol.* **27**, 1334–1347. https://doi.org/10.1128/MCB.01909-06 (2007).
31. Sin, W. C. *et al.* G protein-coupled receptors GPR4 and TDAG8 are oncogenic and overexpressed in human cancers. *Oncogene* **23**, 6299–6303. https://doi.org/10.1038/sj.onc.1207838 (2004).
32. Jing, Z. *et al.* The proton-sensing G-protein coupled receptor gpr4 promotes angiogenesis in head and neck cancer. *PLoS ONE* **11**, e0152789. https://doi.org/10.1371/journal.pone.0152789 (2016).
33. Ihara, Y. *et al.* The G protein-coupled receptor T-cell death-associated gene 8 (TDAG8) facilitates tumor development by serving as an extracellular pH sensor. *Proc. Natl. Acad. Sci. USA* **107**, 17309–17314. https://doi.org/10.1073/pnas.1001165107 (2010).
34. Im, D. S., Heise, C. E., Nguyen, T., O'Dowd, B. F. & Lynch, K. R. Identification of a molecular target of psychosine and its role in globoid cell formation. *J. Cell. Biol.* **153**, 429–434. https://doi.org/10.1083/jcb.153.2.429 (2001).
35. Malone, M. H., Wang, Z. & Distelhorst, C. W. The glucocorticoid-induced gene tdag8 encodes a pro-apoptotic G protein-coupled receptor whose activation promotes glucocorticoid-induced apoptosis. *J. Biol. Chem.* **279**, 52850–52859. https://doi.org/10.1074/jbc.M408040200 (2004).
36. Nagasaka, A. *et al.* The proton-sensing G protein-coupled receptor T-cell death-associated gene 8 (TDAG8) shows cardioprotective effects against myocardial infarction. *Sci. Rep.* **7**, 7812. https://doi.org/10.1038/s41598-017-07573-2 (2017).
37. Onozawa, Y., Komai, T. & Oda, T. Activation of T cell death-associated gene 8 attenuates inflammation by negatively regulating the function of inflammatory cells. *Eur. J. Pharmacol.* **654**, 315–319. https://doi.org/10.1016/j.ejphar.2011.01.005 (2011).
38. Tcymbarevich, I. *et al.* Lack of the pH-sensing receptor TDAG8 [GPR65] in macrophages plays a detrimental role in murine models of inflammatory bowel disease. *J. Crohns Colitis* **13**, 245–258. https://doi.org/10.1093/ecco-jcc/jjy152 (2019).
39. Li, J. *et al.* Ovarian cancer G protein coupled receptor 1 suppresses cell migration of MCF7 breast cancer cells via a Galpha12/13-Rho-Rac1 pathway. *J Mol Signal* **8**, 6. https://doi.org/10.1186/1750-2187-8-6 (2013).
40. Li, H. *et al.* Correction: Abnormalities in osteoclastogenesis and decreased tumorigenesis in mice deficient for ovarian cancer g protein-coupled receptor 1. *PLoS ONE* **10**, e0125463. https://doi.org/10.1371/journal.pone.0125463 (2015).
41. Yan, L., Singh, L. S., Zhang, L. & Xu, Y. Role of OGR1 in myeloid-derived cells in prostate cancer. *Oncogene* **33**, 157–164. https://doi.org/10.1038/onc.2012.566 (2014).
42. de Valliere, C. *et al.* G protein-coupled pH-sensing receptor OGR1 is a regulator of Intestinal inflammation. *Inflamm. Bowel Dis* **21**, 1269–1281. https://doi.org/10.1097/MIB.0000000000000375 (2015).
43. Ichimonji, I. *et al.* Extracellular acidification stimulates IL-6 production and Ca(2+) mobilization through proton-sensing OGR1 receptors in human airway smooth muscle cells. *Am. J. Physiol. Lung Cell. Mol. Physiol.* **299**, L567-577. https://doi.org/10.1152/ajplung.00415.2009 (2010).
44. Matsuzaki, S. *et al.* Extracellular acidification induces connective tissue growth factor production through proton-sensing receptor OGR1 in human airway smooth muscle cells. *Biochem. Biophys. Res. Commun.* **413**, 499–503. https://doi.org/10.1016/j.bbrc.2011.08.087 (2011).
45. Tomura, H. *et al.* Prostaglandin I(2) production and cAMP accumulation in response to acidic extracellular pH through OGR1 in human aortic smooth muscle cells. *J. Biol. Chem.* **280**, 34458–34464. https://doi.org/10.1074/jbc.M505287200 (2005).
46. Obinata, H. & Izumi, T. G2A as a receptor for oxidized free fatty acids. *Prostaglandins Other Lipid Mediat.* **89**, 66–72. https://doi.org/10.1016/j.prostaglandins.2008.11.002 (2009).
47. Okajima, F. Regulation of inflammation by extracellular acidification and proton-sensing GPCRs. *Cell Signal* **25**, 2263–2271. https://doi.org/10.1016/j.cellsig.2013.07.022 (2013).
48. Weng, Z. *et al.* A DNA damage and stress inducible G protein-coupled receptor blocks cells in G2/M. *Proc. Natl. Acad. Sci. USA* **95**, 12334–12339. https://doi.org/10.1073/pnas.95.21.12334 (1998).
49. Le, L. Q. *et al.* Mice lacking the orphan G protein-coupled receptor G2A develop a late-onset autoimmune syndrome. *Immunity* **14**, 561–571 (2001).

50. Zohn, I. E. *et al.* G2A is an oncogenic G protein-coupled receptor. *Oncogene* **19**, 3866–3877. https://doi.org/10.1038/sj.onc.1203731 (2000).
51. Hattori, T. *et al.* G2A plays proinflammatory roles in human keratinocytes under oxidative stress as a receptor for 9-hydroxyoctadecadienoic acid. *J. Invest. Dermatol.* **128**, 1123–1133. https://doi.org/10.1038/sj.jid.5701172 (2008).

Acknowledgements
The study was supported by German Research Foundation (DFG) grant SCHR 1288/6-1.

Author contributions
W.K. performed experiments, evaluated stained samples, interpreted the data and wrote parts of the manuscript. S.W. performed experiments and evaluated samples. C.B. evaluated and categorized tumor tissue samples. J.A.S. and S.S. interpreted the data and wrote parts of the manuscript and finalized the paper. S.S. designed research and obtained grant support (German Research Foundation, SCHR 1288/6-1). J.A.S. and S.S. are equal supervising authors. All authors have read the manuscript and approved the final version.

Funding
Open Access funding provided by Projekt DEAL.

Competing interests
The authors declare no competing interests.

Additional information
Supplementary information is available for this paper at https://doi.org/10.1038/s41598-020-71700-9.

Correspondence and requests for materials should be addressed to S.S.

Reprints and permissions information is available at www.nature.com/reprints.

Publisher's note Springer Nature remains neutral with regard to jurisdictional claims in published maps and institutional affiliations.

Supplementary Information

Expression profiles of Proton-sensing G-Protein coupled receptors in common skin tumors

Wybke Klatt, Susanne Wallner, Christoph Brochhausen, Judith A. Stolwijk, Stephan Schreml*

Supplementary Figures

Figure S1

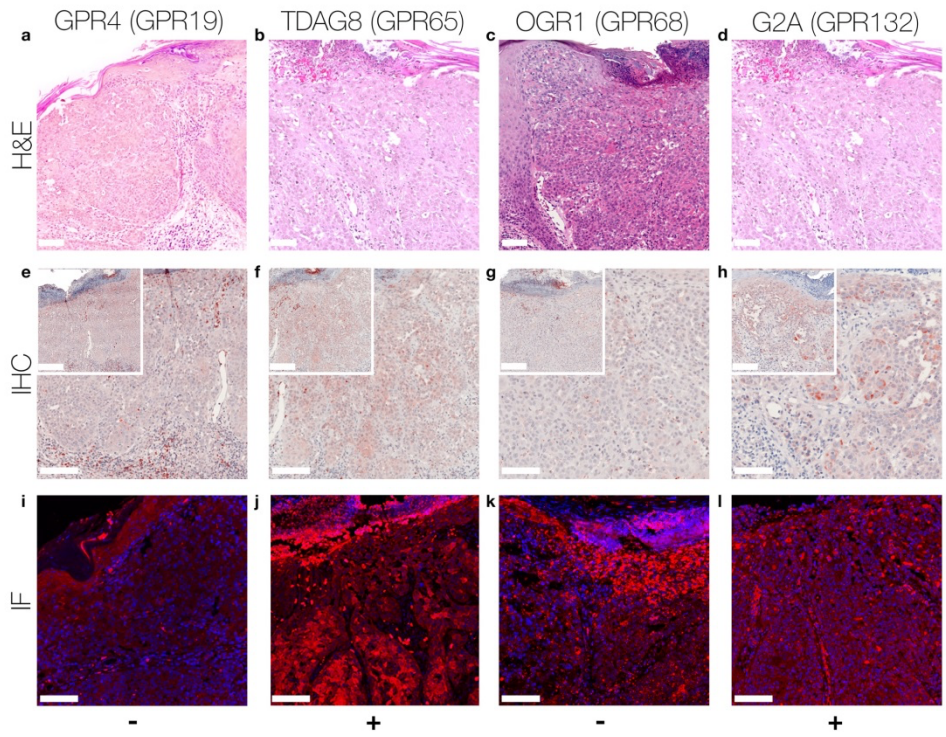

Figure S1: Immunohistochemistry and Immunofluorescence of SCC.
Immunohistochemical and immunofluorescent staining for GPR4 (GPR19), TDAG8 (GPR65), OGR1 (GPR68) and G2A (GPR132) in SCC tissue. (a-d) histochemical H&E staining, (e-h) immunohistochemical staining, inserted images present a 2x larger field of view, (i-l) immunofluorescence staining, red: secondary antibody label, blue: DAPI. Scale bars correspond to 100 µm (a-l: patient 2). Scores (bottom row) were assigned for ++: strong positive/positive reactions; +: weak positive/partial positive reaction; -: negative reaction. The SCC shows no expression of GPR4 and OGR1. There is a weak positive expression of TDAG8 and G2A.

Figure S2

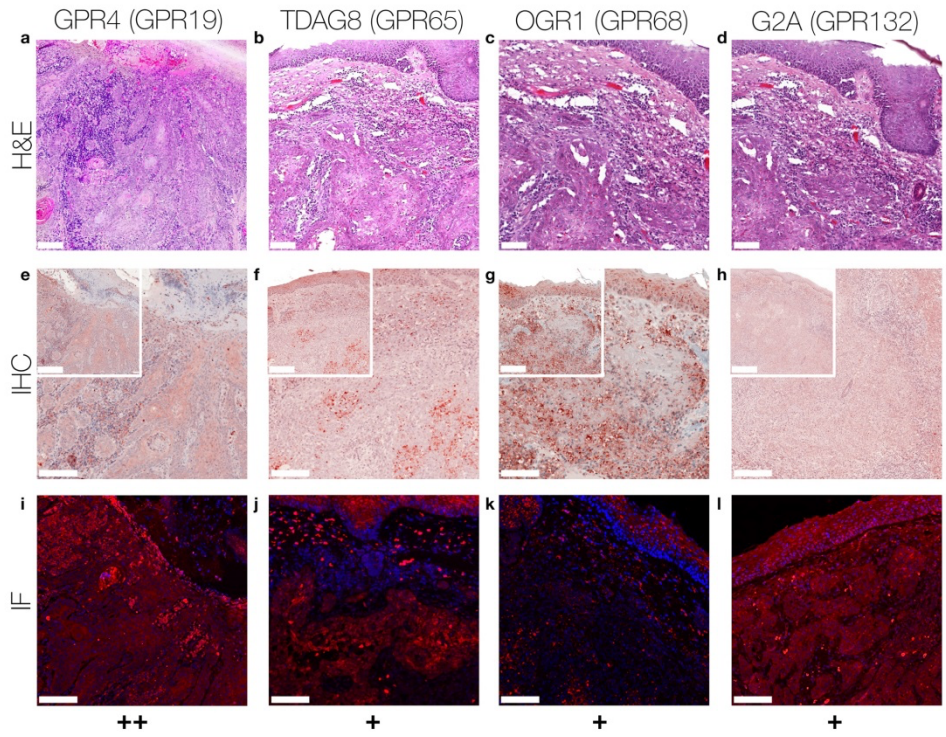

Figure S2: Immunohistochemistry and Immunofluorescence of SCC.
Immunohistochemical and immunofluorescent staining for GPR4 (GPR19), TDAG8 (GPR65), OGR1 (GPR68) and G2A (GPR132) in SCC tissue. (a-d) histochemical H&E staining, (e-h) immunohistochemical staining, inserted images present a 2x larger field of view, (i-l) immunofluorescence staining, red: secondary antibody label, blue: DAPI. Scale bars correspond to 100 μm (a, e, i: patient 1; b, c, d, f, g, h, j, k, l: patient 3). Scores (bottom row) were assigned for ++: strong positive/positive reactions; +: weak positive/partial positive reaction; -: negative reaction. The SCC shows a weak positive expression of TDAG8, OGR1 and G2A. GPR4 is expressed strongly on tumour cells.

Figure S3

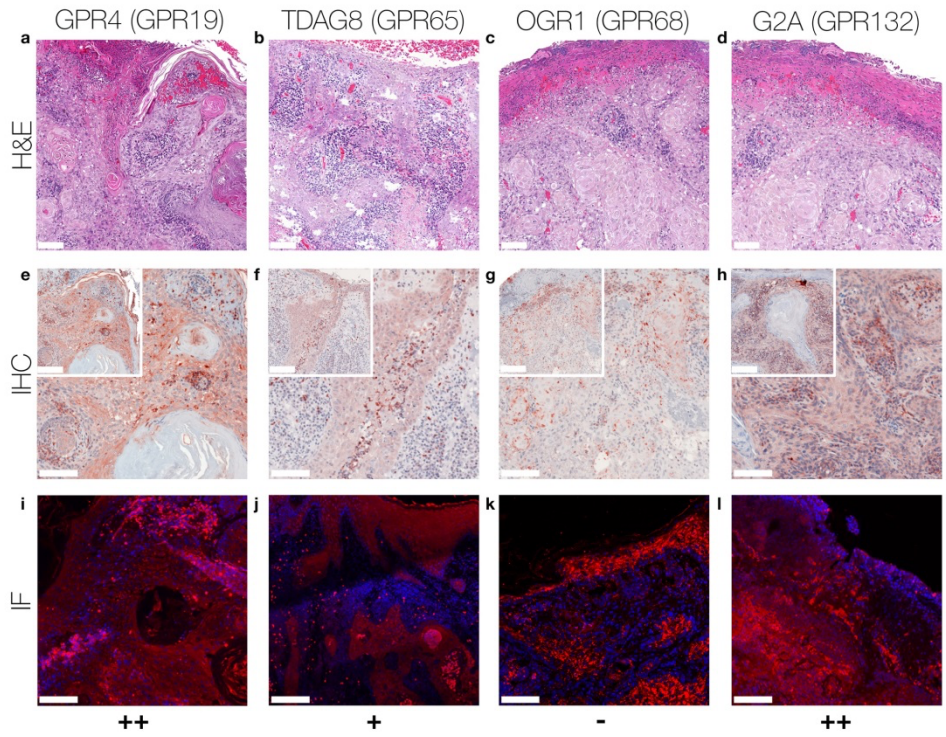

Figure S3: Immunohistochemistry and Immunofluorescence of SCC.
Immunohistochemical and immunofluorescent staining for GPR4 (GPR19), TDAG8 (GPR65), OGR1 (GPR68) and G2A (GPR132) in SCC tissue. (a-d) histochemical H&E staining, (e-h) immunohistochemical staining, inserted images present a 2x larger field of view, (i-l) immunofluorescence staining, red: secondary antibody label, blue: DAPI. Scale bars correspond to 100 μm (a, c, d, e, g, h, i, k, l: patient 4, b, f, j: patient 5). Scores (bottom row) were assigned for ++: strong positive/positive reactions; +: weak positive/partial positive reaction; -: negative reaction. The SCC shows no expression of OGR1. The tumor cells show a partial positive expression of TDAG8. The expression of GPR4 and G2A is significantly increased on tumor cells.

Figure S4

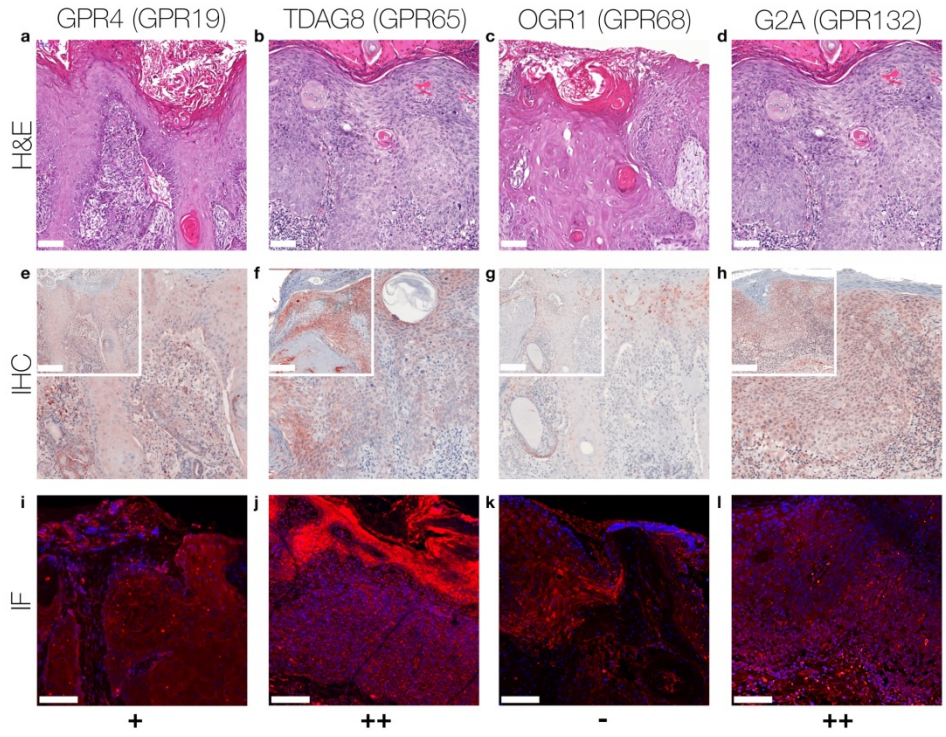

Figure S4: Immunohistochemistry and Immunofluorescence of SCC.
Immunohistochemical and immunofluorescent staining for GPR4 (GPR19), TDAG8 (GPR65), OGR1 (GPR68) and G2A (GPR132) in SCC tissue. (a-d) histochemical H&E staining, (e-h) immunohistochemical staining, inserted images present a 2x larger field of view, (i-l) immunofluorescence staining, red: secondary antibody label, blue: DAPI. Scale bars correspond to 100 μm (a, c, e, g, i: patient 6; b, d, f, h, j, l: patient 7). Scores (bottom row) were assigned for ++: strong positive/positive reactions; +: weak positive/partial positive reaction; -: negative reaction. The SCC shows no expression of OGR1 and a weak positive expression of GPR4. It shows a significantly increased expression of TDAG8 and G2A on the surface of tumor cells.

Figure S5

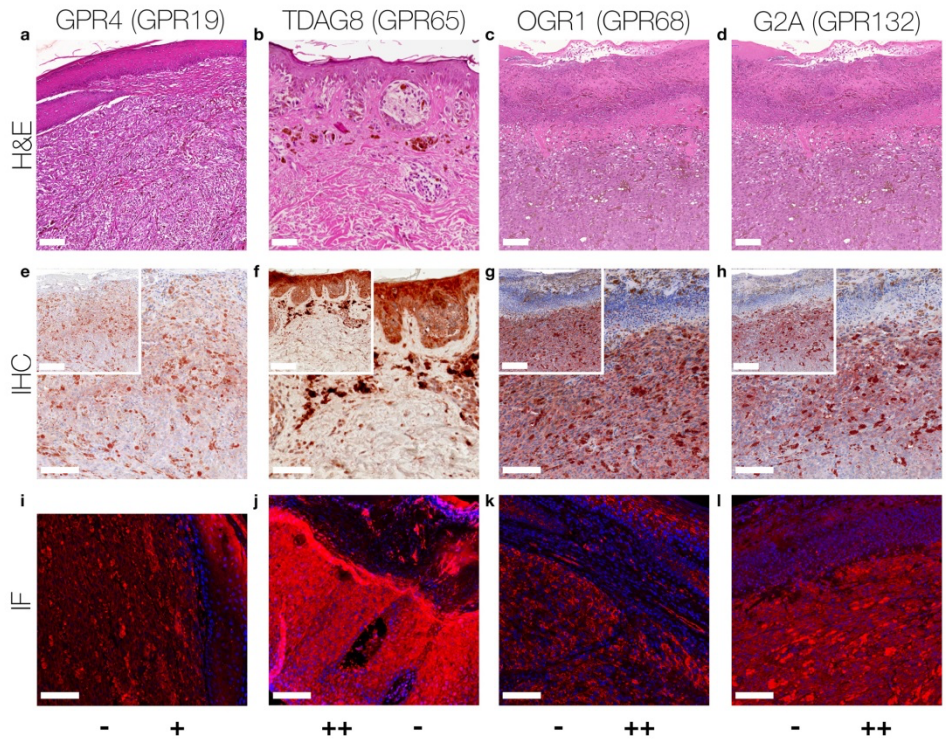

Figure S5: Immunohistochemistry and Immunofluorescence of MM.
Immunohistochemical and immunofluorescent staining for GPR4 (GPR19), TDAG8 (GPR65), OGR1 (GPR68) and G2A (GPR132) in MM tissue. (a-d) histochemical H&E staining, (e-h) immunohistochemical staining, inserted images present a 2x larger field of view, (i-l) immunofluorescence staining, red: secondary antibody label, blue: DAPI. Scale bars correspond to 100 μm (b, f, j: patient 10; a, c, d, e, g, h, k, i, l: patient 11). Scores (bottom row) were assigned for ++: strong positive/positive reactions; +: weak positive/partial positive reaction; -: negative reaction for the epidermal (left score) and the dermal (right score) region. The MM shows no expression on the epidermal regions of GPR4, OGR1 and G2A as well as there is a strong expression on the epidermal part of TDAG8. GPR4 is expressed weakly in the dermis, whereas TDAG8 is not expressed in this section. The dermis of OGR1 and G2A is strongly expressed. It has to be mentioned, that especially in those last two mentioned GPCRs smaller tumor cells appear to be weak positive and multinuclear giant cells are expressed more strong.

Figure S6

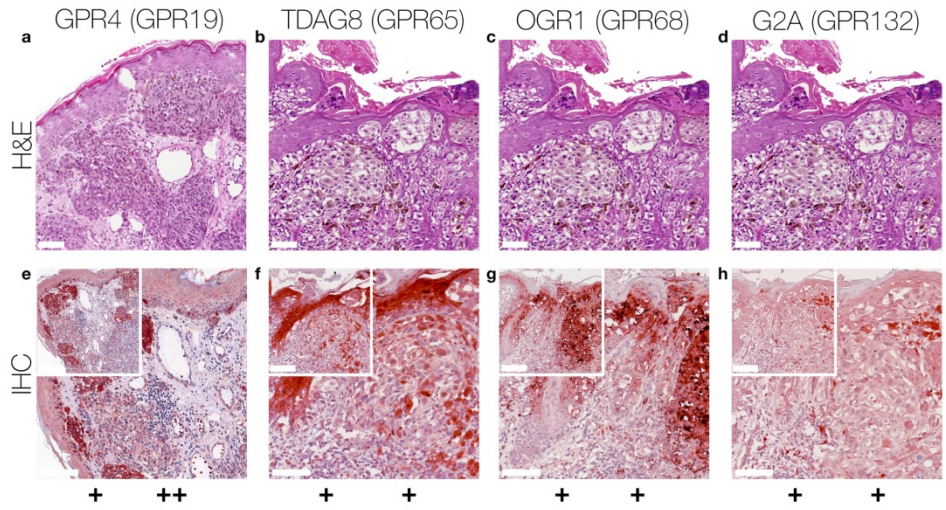

Figure S6: Immunohistochemistry and of MM.
Immunohistochemical and immunofluorescent staining for GPR4 (GPR19), TDAG8 (GPR65), OGR1 (GPR68) and G2A (GPR132) in MM tissue. (a-d) histochemical H&E staining, (e-h) immunohistochemical staining, inserted images present a 2x larger field of view. Scale bars correspond to 100 μm (a-l: patient 12). Scores (bottom row) were assigned for ++: strong positive/positive reactions; +: weak positive/partial positive reaction; -: negative reaction for the epidermal (left score) and the dermal (right score) region. The MM shows a partial positive expression on the epidermal and dermal regions of TDAG8, OGR1 and G2A. GPR4 is expressed weakly in the epidermis, but strongly in the dermis. Some tumor nest are only weakly coloured, others with multinuclear giant cells are expressed strongly.

Figure S7

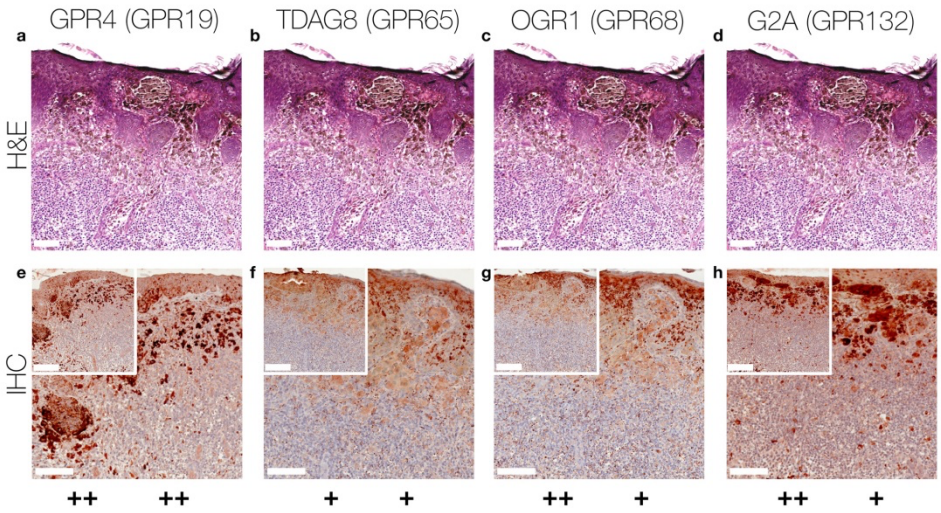

Figure S7: Immunohistochemistry of MM.
Immunohistochemical and immunofluorescent staining for GPR4 (GPR19), TDAG8 (GPR65), OGR1 (GPR68) and G2A (GPR132) in SCC tissue. (a-d) histochemical H&E staining, (e-h) immunohistochemical staining, inserted images present a 2x larger field of view (a-l: patient 13). Scores (bottom row) were assigned for ++: strong positive/positive reactions; +: weak positive/partial positive reaction; -: negative reaction for the epidermal (left score) and the dermal (right score) region. There is a strong positive epidermal expression of GPR4, OGR1 and G2A detected. TDAG8 is weak positive epidermally. The dermal expression of TDAG8, OGR1 and G2A is partial positive, but the GPR4 is expressed strongly in the dermal area. Smaller tumor cells within the tumor appear to be weak positive, whereas multinuclear giant tumor cells are strongly expressed.

Figure S8

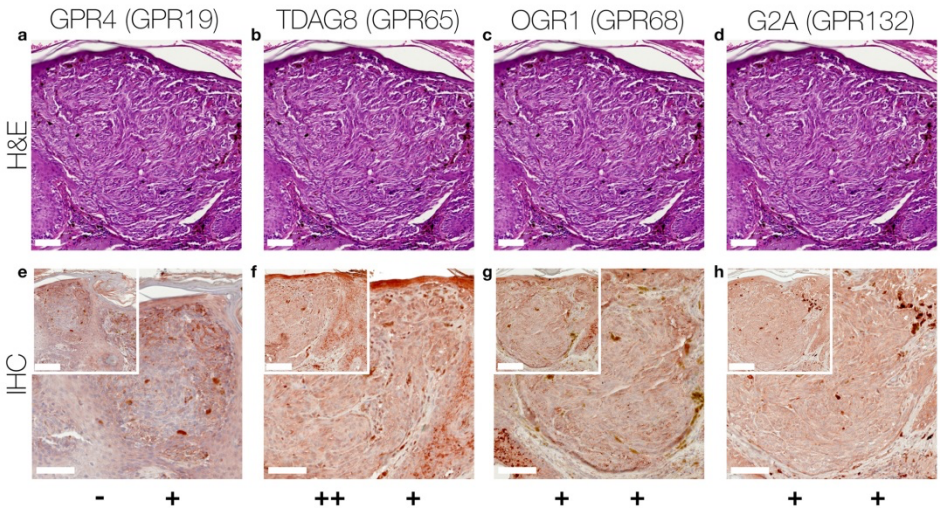

Figure S8: Immunohistochemistry of MM.
Immunohistochemical and immunofluorescent staining for GPR4 (GPR19), TDAG8 (GPR65), OGR1 (GPR68) and G2A (GPR132) in MM tissue. (a-d) histochemical H&E staining, (e-h) immunohistochemical staining, inserted images present a 2x larger field of view (a-l: patient 14). Scores (bottom row) were assigned for ++: strong positive/positive reactions; +: weak positive/partial positive reaction; -: negative reaction for the epidermal (left score) and the dermal (right score) region. The MM shows no epidermal expression of GPR4, but TDAG8 is strongly expressed in the epidermis. OGR1 and G2A are partial positive regarding the epidermis. All four GPCRs are expressed partially in the dermis. Smaller tumor cells within the tumor appear to be weak positive, while multinuclear giant tumor cells with altered nucleus-cytoplasmic ratio are strongly expressed.

Figure S9

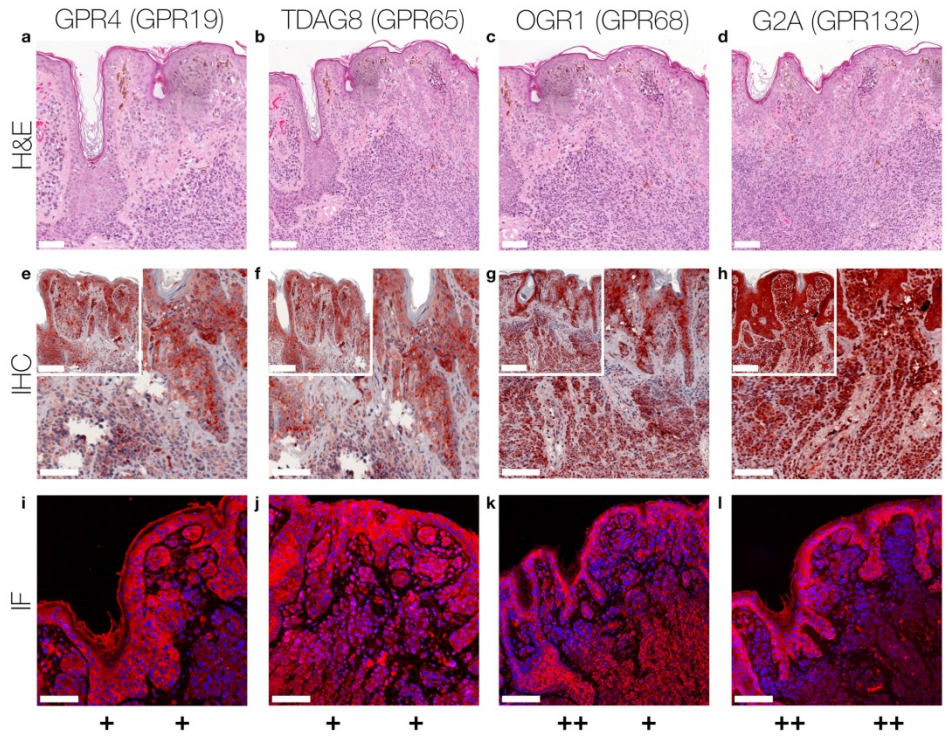

Figure S9: Immunohistochemistry and Immunofluorescence of NCN.
Immunohistochemical and immunofluorescent staining for GPR4 (GPR19), TDAG8 (GPR65), OGR1 (GPR68) and G2A (GPR132) in NCN tissue. (a-d) histochemical H&E staining, (e-h) immunohistochemical staining, inserted images present a 2x larger field of view, (i-l) immunofluorescence staining, red: secondary antibody label, blue: DAPI. Scale bars correspond to 100 μm (a-l: patient 16). Scores (bottom row) were assigned for ++: strong positive/positive reactions; +: weak positive/partial positive reaction; -: negative reaction for the epidermal (left score) and the dermal (right score) region. The NCN shows a strong positive expression on the epidermal regions of OGR1 and G2A. The epidermal expression of GPR4 and TDAG8 is partial positive. Besides the strong positive dermal expression of GPR132, the other three receptors GPR4, TDAG8 and OGR1 are weak positive in the dermis.

Figure S10

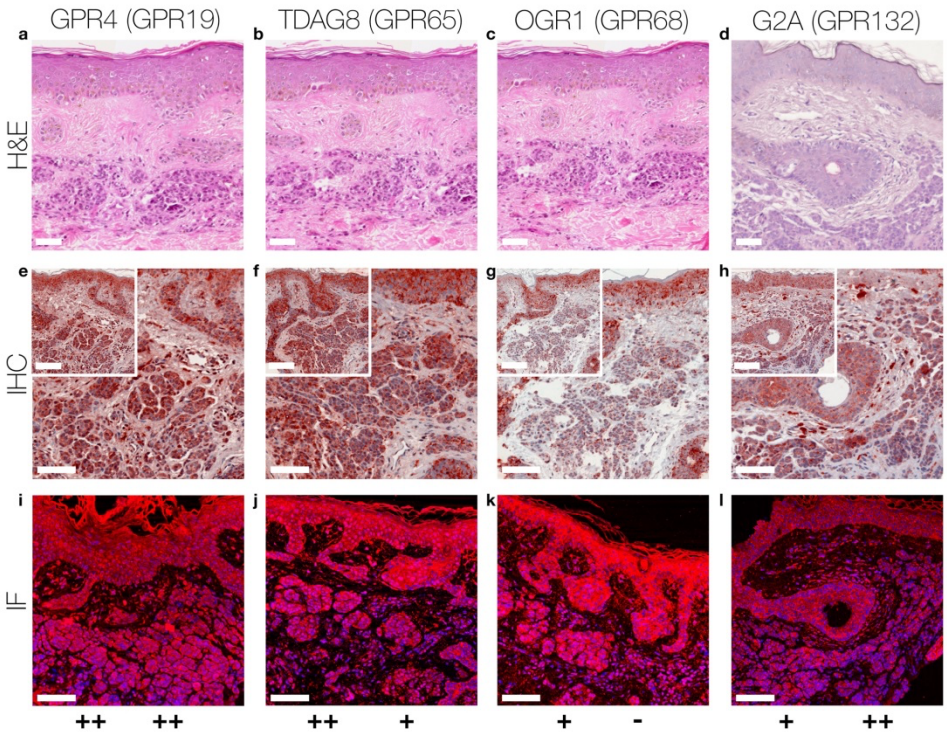

Figure S10: Immunohistochemistry and Immunofluorescence of NCN.
Immunohistochemical and immunofluorescent staining for GPR4 (GPR19), TDAG8 (GPR65), OGR1 (GPR68) and G2A (GPR132) in NCN tissue. (a-d) histochemical H&E staining, (e-h) immunohistochemical staining, inserted images present a 2x larger field of view, (i-l) immunofluorescence staining, red: secondary antibody label, blue: DAPI. Scale bars correspond to 100 μm (a-l: patient 17). Scores (bottom row) were assigned for ++: strong positive/positive reactions; +: weak positive/partial positive reaction; -: negative reaction for the epidermal (left score) and the dermal (right score) region. The epidermal expression of GPR4 and TDAG8 is significantly increased on NCN. There is a weak expression of OGR1 and G2A in the epidermis. In contrast, there is no dermal expression of OGR1 and only a weak expression of TDAG8. GPR4 and G2A are significantly expressed with an overall stronger expression on multinuclear giant cells in the dermis than smaller tumor cells within the tumor.

Figure S11

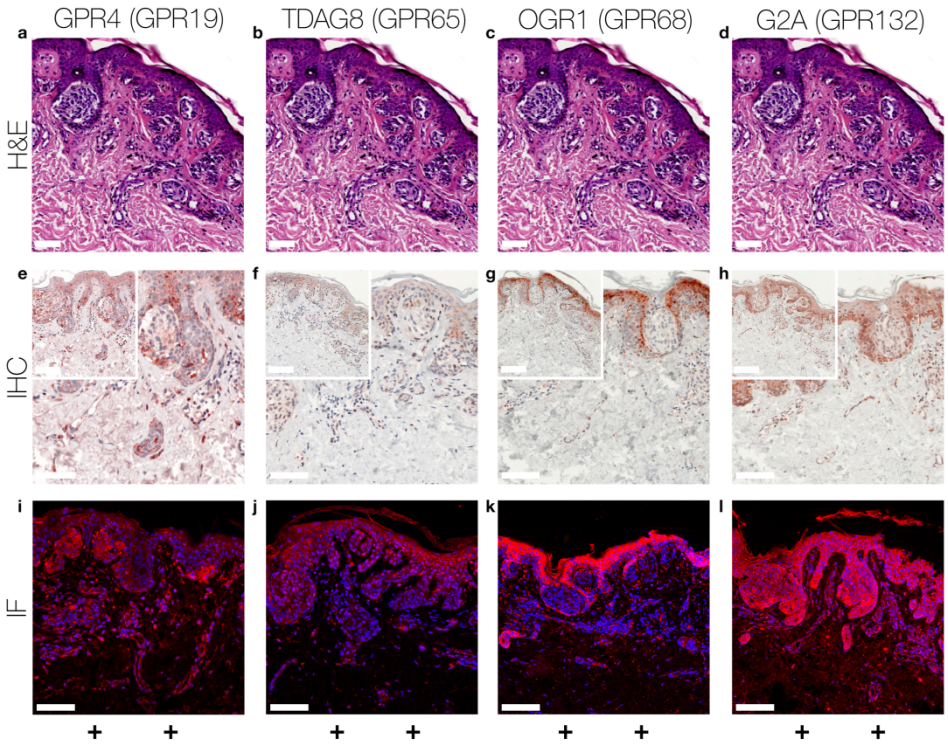

Figure S11: Immunohistochemistry and Immunofluorescence of NCN.
Immunohistochemical and immunofluorescent staining for GPR4 (GPR19), TDAG8 (GPR65), OGR1 (GPR68) and G2A (GPR132) in NCN tissue. (a-d) histochemical H&E staining, (e-h) immunohistochemical staining, inserted images present a 2x larger field of view, (i-l) immunofluorescence staining, red: secondary antibody label, blue: DAPI. Scale bars correspond to 100 μm (a-l: patient 18). Scores (bottom row) were assigned for ++: strong positive/positive reactions; +: weak positive/partial positive reaction; -: negative reaction for the epidermal (left score) and the dermal (right score) region. The NCN sample shows a weak positive epidermal as well as dermal expression of all four GPCRs. Especially in the dermal part of GPR4 smaller tumor cells within the tumor appear to be weak positive for GPR4 and multinuclear giant tumor cells with altered nucleus-cytoplasmic ratio strongly express GPR4.

Figure S12

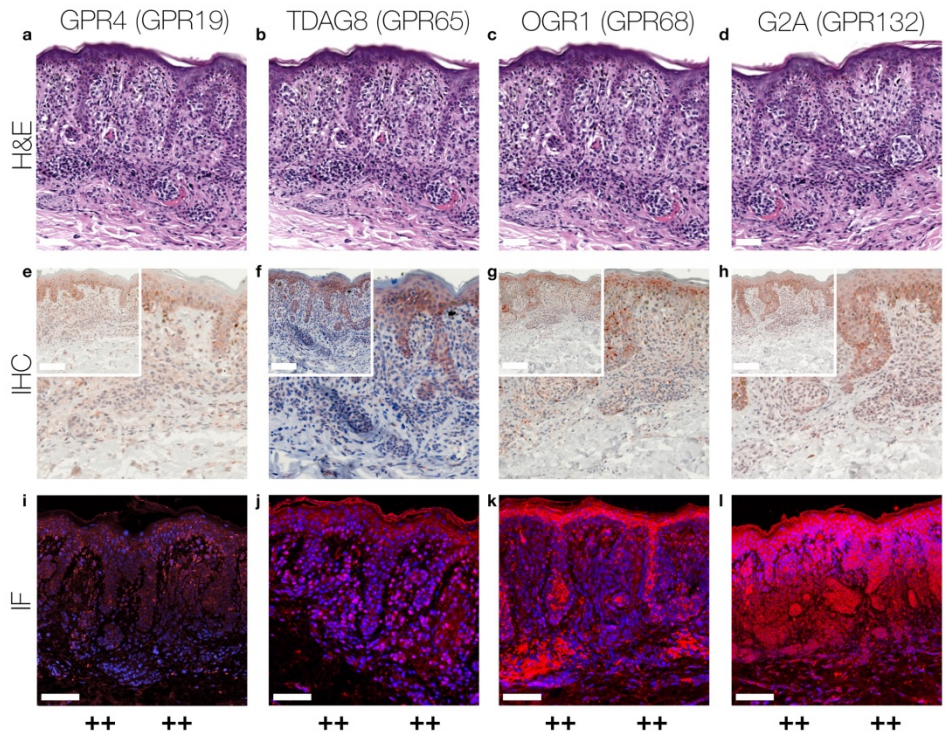

Figure S12: Immunohistochemistry and Immunofluorescence of NCN.
Immunohistochemical and immunofluorescent staining for GPR4 (GPR19), TDAG8 (GPR65), OGR1 (GPR68) and G2A (GPR132) in NCN tissue. (a-d) histochemical H&E staining, (e-h) immunohistochemical staining, inserted images present a 2x larger field of view, (i-l) immunofluorescence staining, red: secondary antibody label, blue: DAPI. Scale bars correspond to 100 μm (a-l: patient 19). Scores (bottom row) were assigned for ++: strong positive/positive reactions; +: weak positive/partial positive reaction; -: negative reaction for the epidermal (left score) and the dermal (right score) region. The NCN shows a strong positive epidermal as well as dermal expression of all four GPCRs.

Figure S13

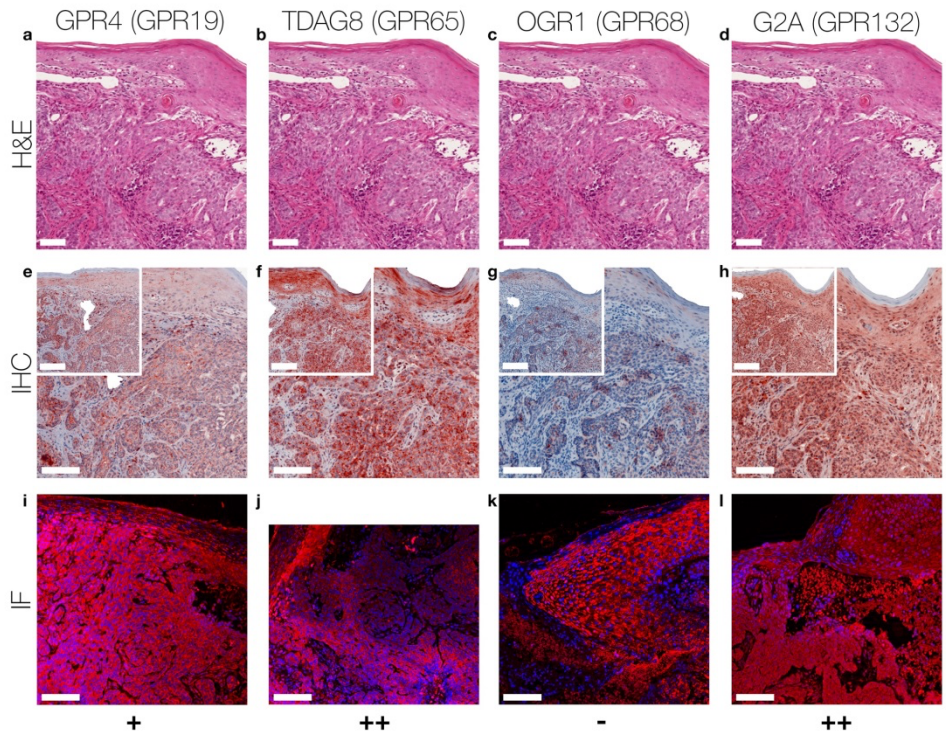

Figure S13: Immunohistochemistry and Immunofluorescence of BCC.
Immunohistochemical and immunofluorescent staining for GPR4 (GPR19), TDAG8 (GPR65), OGR1 (GPR68) and G2A (GPR132) in BCC tissue. (a-d) histochemical H&E staining, (e-h) immunohistochemical staining, inserted images present a 2x larger field of view, (i-l) immunofluorescence staining, red: secondary antibody label, blue: DAPI. Scale bars correspond to 100 µm (a-l: patient 21). Scores (bottom row) were assigned for ++: strong positive/positive reactions; +: weak positive/partial positive reaction; -: negative reaction. The expression of TDAG8 and G2A is significantly increased on BCC. The BCC shows a weak positive expression of GPR4.There is no expression of OGR1.

Figure S14

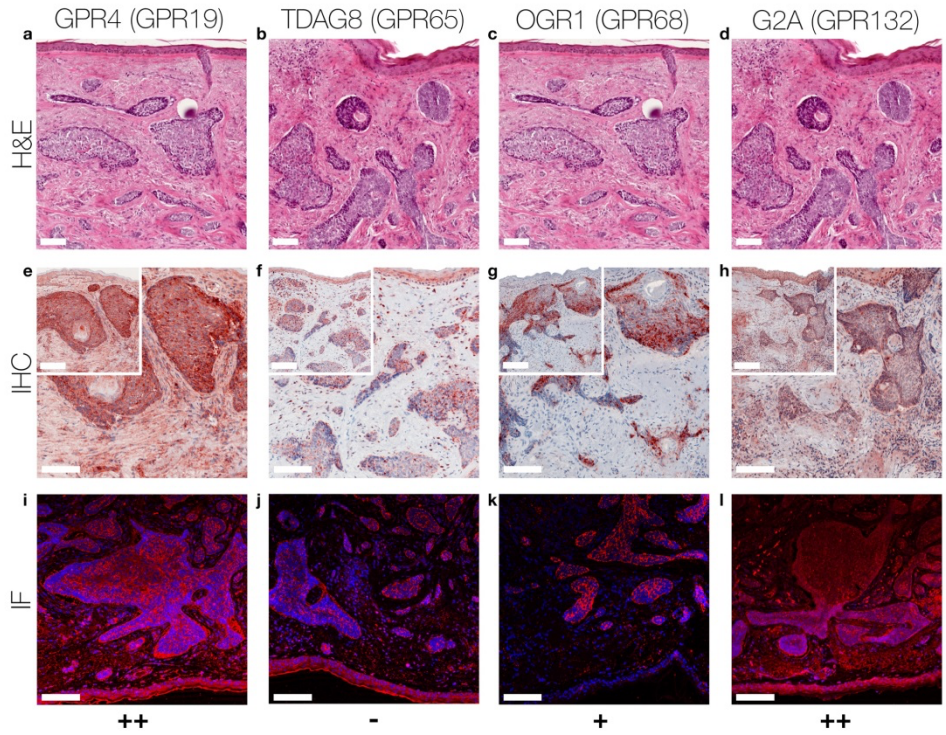

Figure S14: Immunohistochemistry and Immunofluorescence of BCC.
Immunohistochemical and immunofluorescent staining for GPR4 (GPR19), TDAG8 (GPR65), OGR1 (GPR68) and G2A (GPR132) in BCC tissue. (a-d) histochemical H&E staining, (e-h) immunohistochemical staining, inserted images present a 2x larger field of view, (i-l) immunofluorescence staining, red: secondary antibody label, blue: DAPI. Scale bars correspond to 100 µm (a-l: patient 22). Scores (bottom row) were assigned for ++: strong positive/positive reactions; +: weak positive/partial positive reaction; -: negative reaction. The BCC shows on the one hand a significantly increased expression of GPR4 as well as G2A and on the other hand a weak positive expression of OGR1. In contrast, there is no expression of TDAG8, only several peritumoral lymphocytes appear to be positive.

Figure S15

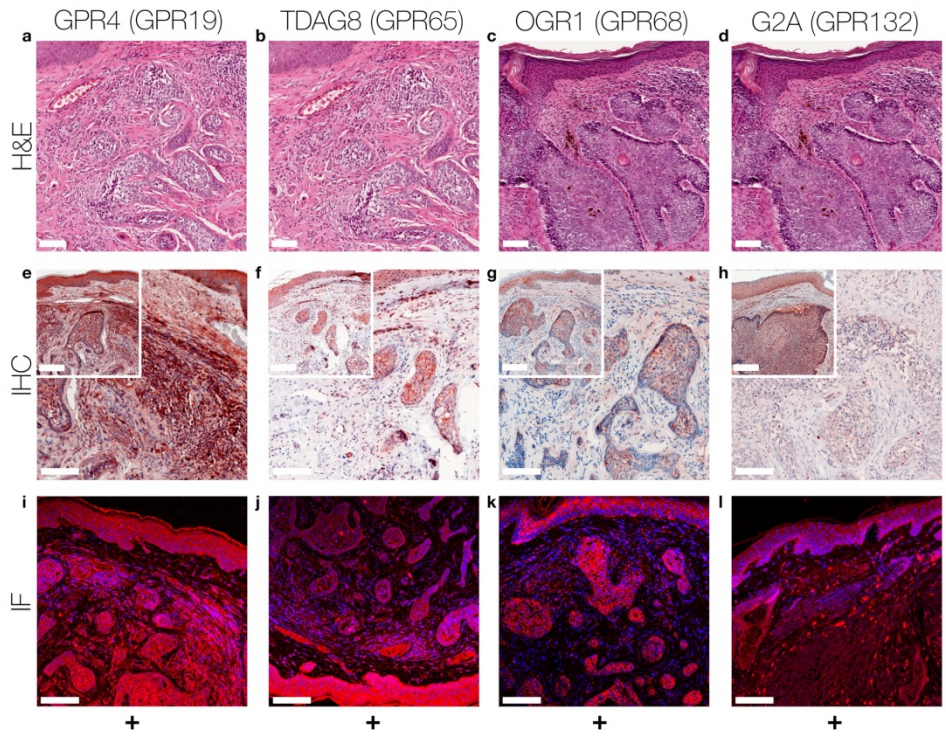

Figure S15: Immunohistochemistry and Immunofluorescence of BCC.
Immunohistochemical and immunofluorescent staining for GPR4 (GPR19), TDAG8 (GPR65), OGR1 (GPR68) and G2A (GPR132) in BCC tissue. (a-d) histochemical H&E staining, (e-h) immunohistochemical staining, inserted images present a 2x larger field of view, (i-l) immunofluorescence staining, red: secondary antibody label, blue: DAPI. Scale bars correspond to 100 µm (a-l: patient 23). Scores (bottom row) were assigned for ++: strong positive/positive reactions; +: weak positive/partial positive reaction; -: negative reaction. The BCC shows a weak positive expression of all four GPCRs.

Figure S16

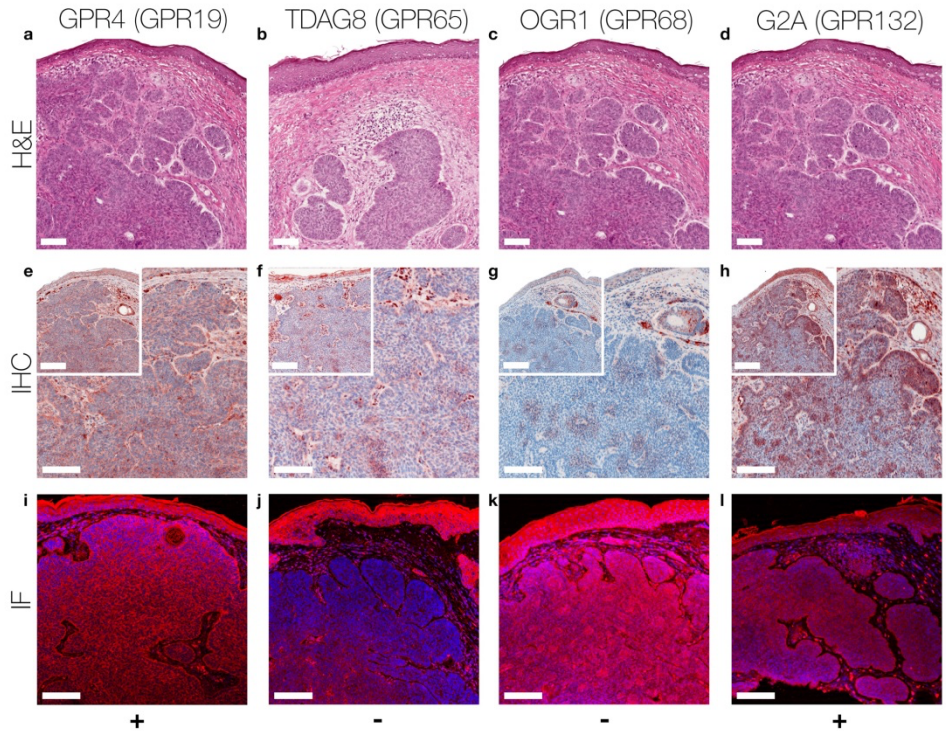

Figure S16: Immunohistochemistry and Immunofluorescence of BCC.
Immunohistochemical and immunofluorescent staining for GPR4 (GPR19), TDAG8 (GPR65), OGR1 (GPR68) and G2A (GPR132) in BCC tissue. (a-d) histochemical H&E staining, (e-h) immunohistochemical staining, inserted images present a 2x larger field of view, (i-l) immunofluorescence staining, red: secondary antibody label, blue: DAPI. Scale bars correspond to 100 µm (a-l: patient 24). Scores (bottom row) were assigned for ++: strong positive/positive reactions; +: weak positive/partial positive reaction; -: negative reaction. The expression of GPR4 and G2A is weak positive on BCC, even though the tumor cells of G2A in the periphery appear to be strong positive in comparison the tumor cells in the centre. There is no expression of TDAG8 and OGR1.

Figure S17

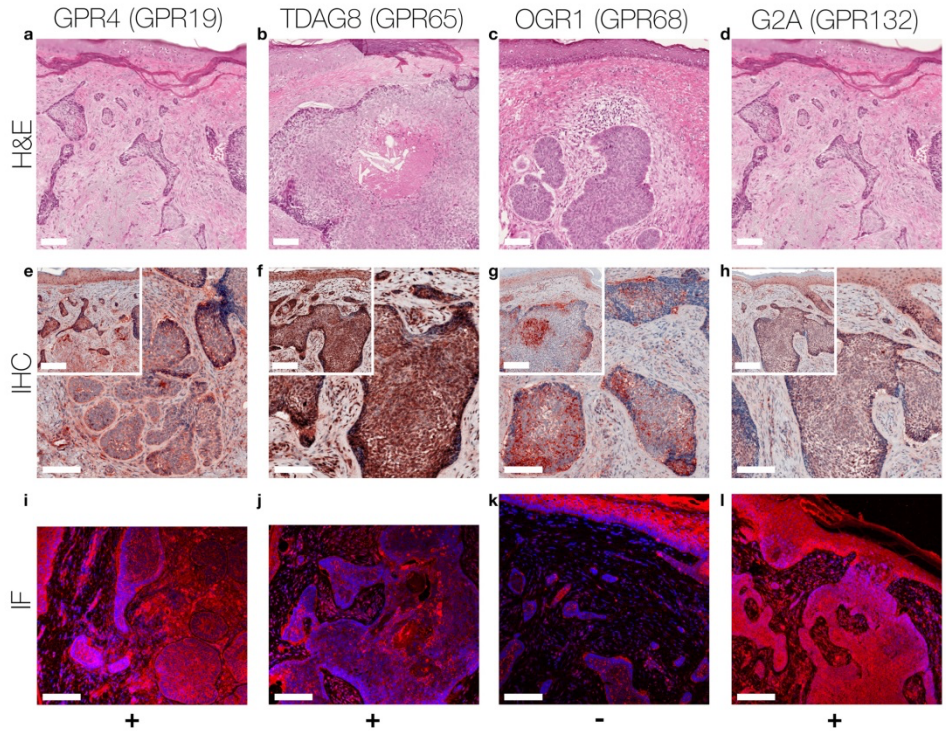

Figure S17: Immunohistochemistry and Immunofluorescence of BCC.
Immunohistochemical and immunofluorescent staining for GPR4 (GPR19), TDAG8 (GPR65), OGR1 (GPR68) and G2A (GPR132) in BCC tissue. (a-d) histochemical H&E staining, (e-h) immunohistochemical staining, inserted images present a 2x larger field of view, (i-l) immunofluorescence staining, red: secondary antibody label, blue: DAPI. Scale bars correspond to 100 µm (a-l: patient 25). Scores (bottom row) were assigned for ++: strong positive/positive reactions; +: weak positive/partial positive reaction; -: negative reaction. Except of the strong positive expressed BCC tumor cells in the periphery of GPR4 and TDAG8, GPR4 as well as TDAG8 and G2A are expressed partial positive. There is no expression of OGR1.

Figure S18

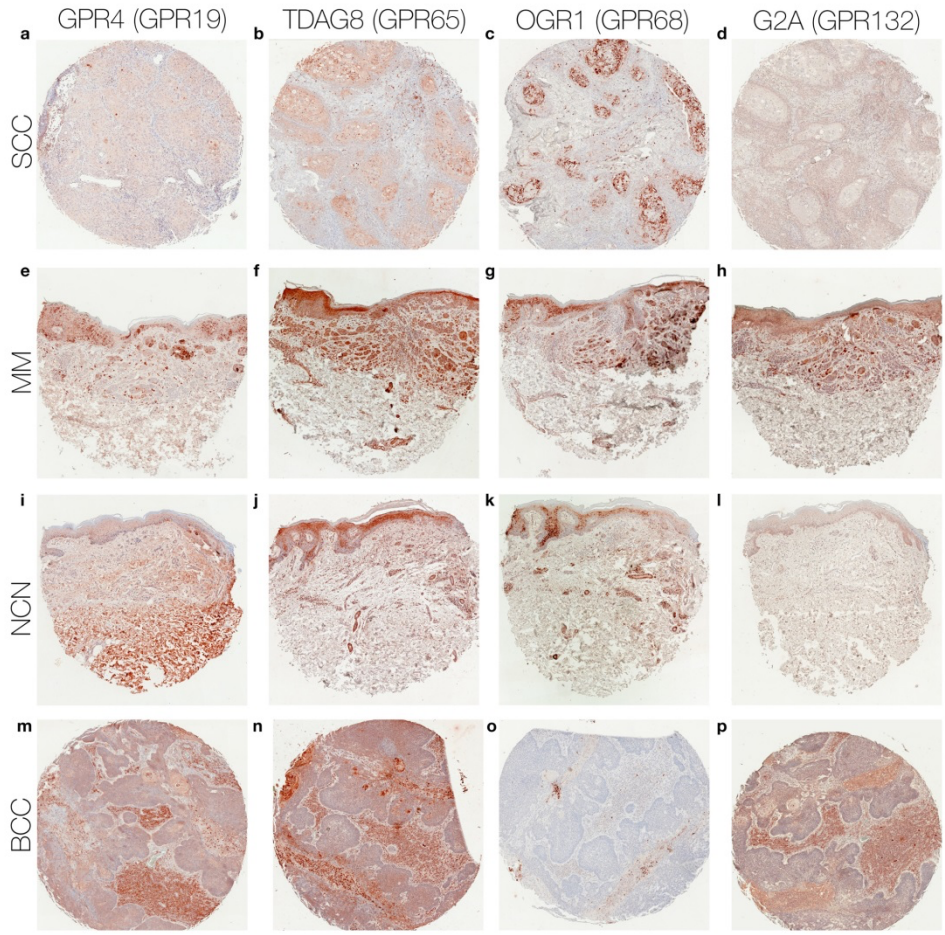

Figure S18: Tissue microarray of SCC, MM, NCN and BCC.
Selection of Immunohistochemical tissue microarray staining for GPR4 (GPR19), TDAG8 (GPR65), OGR1 (GPR68) and G2A (GPR132).

Supplementary tables

Table S1: Overview of general patient data. Overview of age and gender the stained tissue samples were taken from.

patient	gender	age
1	♀	86
2	♂	88
3	♀	85
4	♂	82
5	♀	87
6	♂	90
7	♀	81
8	♂	74
9	♂	34
10	♀	79
11	♀	87
12	♂	69
13	♂	59
14	♂	77
15	♀	68
16	♀	20
17	♂	30
18	♀	49
19	♂	51
20	♂	90
21	♂	90
22	♀	51
23	♂	45
24	♂	84
25	♂	74
26	♂	59
27	♂	80
28	♂	80
29	♂	84
30	♂	74
31	♀	94
32	♀	87
33	♂	73
34	♀	22
35	♀	89
36	♂	51
37	♂	48
38	♂	58
39	♀	66

40	♂	80
41	♂	69
42	♀	45
43	♀	93
44	♀	46
45	♂	69
46	♀	45
47	♀	45
48	♀	74
49	♂	83
50	♀	45
51	♂	83
52	♀	59
53	♂	68
54	♀	36
55	♂	53
56	♂	16
57	♂	55
58	♀	26
59	♀	48
60	♀	59
61	♀	69
62	♂	50
63	♀	69
64	♀	68
65	♂	50
66	♀	33
67	♂	28
68	♀	71
69	♀	27
70	♀	27
71	♀	28
72	♂	85
73	♀	37
74	♀	46
75	♂	69
76	♂	68
77	♂	66
78	♀	44
79	♂	88
80	♀	15
81	♀	50
82	♀	50
83	♀	19

84	♂	27
85	♀	19
86	♀	28
87	♀	43
88	♂	40
89	♂	64
90	♂	10
91	♂	42
92	♀	14
93	♂	38
94	♂	52
95	♀	44
96	♂	38
97	♀	43
98	♀	31
99	♂	11
100	♀	19
101	♀	30
102	♀	8
103	♂	54
104	♀	82
105	♂	77
106	♂	77
107	♂	65
108	♂	64
109	♂	78
110	♂	65
111	♀	65
112	♀	75
113	♀	85
114	♀	83
115	♂	66
116	♂	69
117	♂	98
118	♀	55
119	♀	65
120	♀	71
121	♂	59
122	♀	76
123	♂	69
124	♂	81
125	♂	78
126	♂	83
127	♀	84

Table S2: Scores of SCC. Scores of the staining for GPR4 (GPR19), TDAG8 (GPR65), OGR1 (GPR68) and G2A (GPR132) on SCC cells. ++: strong positive/positive reaction; +: weak positive/ partial positive reaction; -: negative reaction; N/A not available, TMA_{SCC} 1-26: patient 26-51.

TMA_{SCC}	GPR4	TDAG8	OGR1	G2A
1	N/A	N/A	N/A	N/A
2	+	+	+	+
3	+	+	+	+
4	+	+	-	+
5	+	+	-	+
6	+	+	-	+
7	-	+	-	+
8	+	N/A	N/A	-
9	+	+	+	+
10	+	+	-	+
11	+	++	-	-
12	+	+	+	+
13	+	++	++	N/A
14	+	+	+	+
15	+	+	-	+
16	+	+	++	+
17	+	+	+	+
18	++	+	+	++
19	+	+	++	++
20	+	+	N/A	+
21	+	++	+	+
22	+	+	-	+
23	+	N/A	+	+
24	+	+	+	+
25	+	+	-	+
26	+	+	-	+

Table S3: Scores of MM. Scores of the staining for GPR4 (GPR19), TDAG8 (GPR65), OGR1 (GPR68) and G2A (GPR132) on MM cells. ++: strong positive/positive reaction; +: weak positive/ partial positive reaction; -: negative reaction; +N/A not available, TMA_{MM} 1-27: patient 52-78.

TMA_{MM}	GPR4		TDAG8		OGR1		G2A	
	epidermal	dermal	epidermal	dermal	epidermal	dermal	epidermal	dermal
1	N/A	N/A	+ [3]	+ [2]	++	++	+ [3]	++
2	++	- [3]	+ [2]	++	N/A	N/A	++	++
3	++	++	++	++	++	++	++	++
4	++	++ [1]	++	-	++	-	++	+ [1] [3]
5	++	++	++	++	++	+ [2]	++	+ [3]
6	N/A	N/A	+	+	N/A	N/A	N/A	N/A
7	++	++ [1]	+ [3]	+ [2]	++	+ [2]	++	+ [1] [3]
8	++	++ [1]	++	++	++	++ [4]	+	+ [3]
9	++	- [3]	++	++	++	+ [2]	+	+ [3]
10	++	++ [1]	++	+ [2]	++	- [1]	+	+ [1] [3]
11	++	- [2]	++	++	++	++ [4]	+	+
12	N/A	N/A	N/A	N/A	N/A	N/A	+	N/A
13	++	- [2]	++	++	++	++	+	+
14	+	++	++	++	++	++	++	+ [3]
15	++	++	++	++	+	+	+	+ [3]
16	N/A	N/A	N/A	N/A	N/A	N/A	N/A	N/A
17	++	-	+	+	++	+	N/A	N/A
18	N/A	N/A	N/A	N/A	N/A	N/A	N/A	N/A
19	++	+ [2]	++	++	++	+	++	+ [3]
20	++	+ [2]	++	++	++	+ [2]	++	+ [3]
21	++	++ [1]	N/A	N/A	++	+	++	+ [3]
22	N/A	N/A	++	++	++	+	N/A	N/A
23	++	-	++	++	++	+ [2]	+	+
24	N/A	N/A	++	+	++	+ [2]	+	+
25	++	++ [1]	++	++	++	+	++	+ [1] [3]
26	++	+ [3]	++	++	++	+	++	+ [1] [3]
27	N/A	N/A	++	++	++	+	+	+ [3]

[1] strong positive either on the surface or in the deeper parts of the tumor tissue

[2] single tumor cells are strong positive, but the overall impression is weak positive expression

[3] large tumor cells appear to be strong positive

[4] partially strong positive

Table S4: Scores of NCN. Scores of the staining for GPR4 (GPR19), TDAG8 (GPR65), OGR1 (GPR68) and G2A (GPR132) on NCN cells. ++: strong positive/positive reaction; +: weak positive/ partial positive reaction; -: negative reaction; N/A not available, TMA_{NCN} 1-24: patient 79-102

TMA_{NCN}	GPR4		TDAG8		OGR1		G2A	
	epidermal	dermal	epidermal	dermal	epidermal	dermal	epidermal	dermal
1	+	+ [5]	N/A	+ [3]	-	+ [5]	-	+ [2] [5]
2	N/A	+ [5]	+	++	-	+	-	+ [5]
3	+	+ [3] [5]	N/A	N/A	-	+	+ [2]	+ [1] [3]
4	+	+ [3] [5]	N/A	++	-	+ [5]	-	+ [1] [3]
5	++	N/A	N/A	N/A	N/A	N/A	N/A	N/A
6	+	- [3]	+	++	-	+ [5]	+ [2]	+ [2] [5]
7	+	+ [3]	-	++	-	+ [5]	-	++ [4]
8	++	+ [5]	++	++	N/A	N/A	N/A	N/A
9	+	- [3]	+	+ [3]	+ [2]	+	++	- [3]
10	N/A	N/A	+	+	+ [2]	+	+ [2]	+
11	N/A	N/A	N/A	+ [3]	+ [2]	+	N/A	+ [1] [3]
12	N/A	N/A	+	+ [3]	N/A	N/A	-	+
13	+	+ [3]	+	N/A	N/A	N/A	N/A	N/A
14	++	+ [3]	++	++	N/A	N/A	++ [4]	+ [1] [3]
15	+	+ [5]	+	++	-	+	+	+
16	N/A	N/A	+	++	N/A	N/A	N/A	N/A
17	++	N/A	+	+	-	+ [5]	N/A	N/A
18	+	+ [5]	++	++	-	+	+	+ [5]
19	++	N/A	++	N/A	N/A	N/A	++ [4]	N/A
20	++	+ [3] [5]	+	+ [3]	+ [2]	+ [5]	++ [4]	+ [3] [5]
21	N/A	N/A	++	N/A	N/A	N/A	N/A	N/A
22	+	+ [3]	+ [3]	+ [3]	+ [2]	+ [2]	+ [5]	+ [3] [5]
23	++	+	N/A	++	N/A	N/A	N/A	+ [5]
24	+	+ [3] [5]	N/A	++	N/A	+	N/A	+ [3]

[1] strong positive either on the surface or in the deeper parts of the tumor tissue

[2] single tumor cells are strong positive, but the overall impression is weak positive expression

[3] large tumor cells appear to be strong positive

[4] partially strong positive

[5] weak positive

Table S5: Scores of BCC. Scores of the staining for GPR4 (GPR19), TDAG8 (GPR65), OGR1 (GPR68) and G2A (GPR132) on BCC cells. ++: strong positive/positive reaction; +: weak positive/ partial positive reaction; -: negative reaction; N/A not available, TMA_{BCC} 1-25: patient 103-127

TMA_{BCC}	GPR4	TDAG8	OGR1	G2A
1	+ [5)]	+ [5)]	-	++
2	N/A	N/A	N/A	N/A
3	+ [5)]	+ [5)]	+ [6)]	+ [5)]
4	-	+ [5)]	+ [6)]	+ [5)]
5	N/A	+ [6)]	-	N/A
6	+	N/A	+ [6)]	+ [5)]
7	+	+ [5)]	+ [6)]	N/A
8	+	++	+ [6)]	++
9	+	+ [5)]	-	+ [5)]
10	++	+ [5)]	-	++
11	+ [5)]	+ [5)]	-	+ [5)]
12	++	++	+ [6)]	+ [5)]
13	+ [5)]	+ [5)]	+ [5)]	+ [5)]
14	++	N/A	+ [6)]	++
15	++	+ [6)]	-	+ [5)]
16	++	++	+ [6)]	+ [5)]
17	+	++	+ [6)]	N/A
18	++	++	+ [5)]	++
19	+	++	+ [6)]	+ [5)]
20	++	+ [5)]	+ [6)]	++
21	++	++	+ [6)]	++
22	++	++	+	+ [5)]
23	++	++	+ [6)]	+ [5)]
24	++	+ [5)]	+ [6)]	++
25	+ [5)]	+ [5)]	+ [6)]	N/A

[5)] weak positive

[6)] partial positive

Figure S19

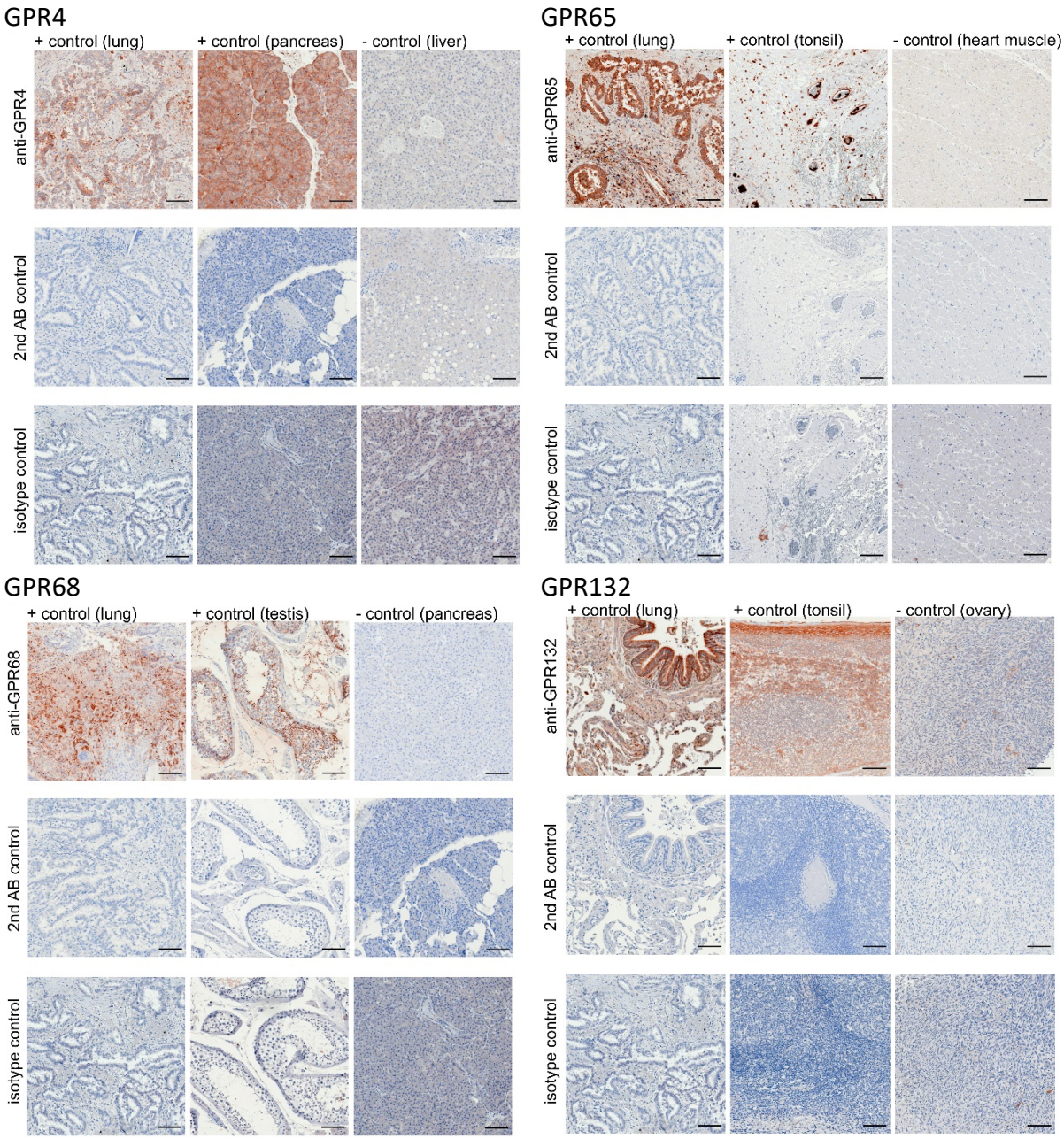

Figure S19: Tissue controls for IHC/TMA staining with anti-pH-GPCR antibodies.
IHC staining on positive and negative control tissue. One positive control tissue was each selected according to the primary antibody datasheet and a second positive control and a negative control for each pH-GPCR were selected according to the proteomics database "The Human Protein Atlas" (www.proteinatlas.org). Control tissue were stained with the respective anti pH-GPCR antibody, the isotype control antibody and without primary antibody (secondary antibody control: 2nd AB control). Scale bars correspond to 100 µm.

Figure S20

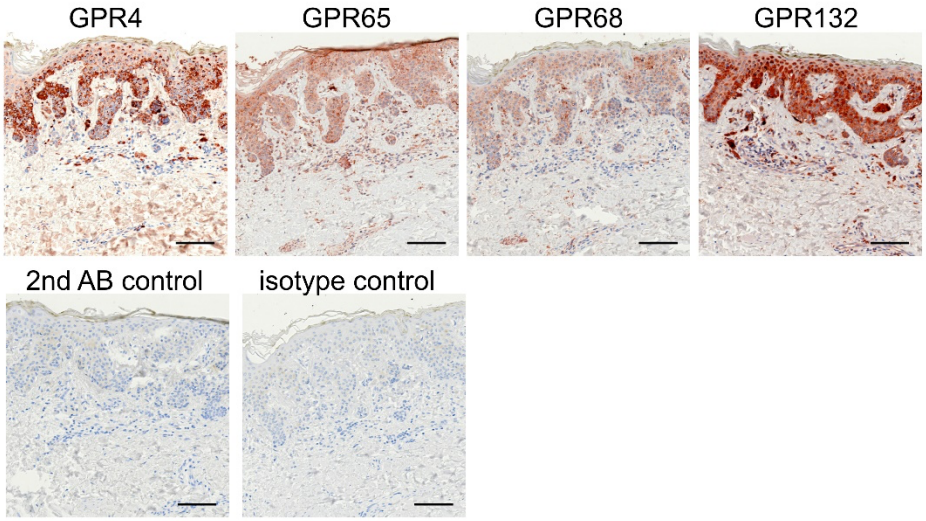

Figure S20: Skin tumor tissue control for IHC/TMA staining with anti-pH-GPCR antibodies. IHC staining on a malignant melanoma tissue section with the four anti-pH-GPCR antibodies, the isotype control antibody and without primary antibody (secondary antibody control: 2nd AB control). Scale bars correspond to 100 µm.

8 Danksagung

Mein Dank gilt all denjenigen, die mich auf dem Weg zum erfolgreichen Abschluss meiner Promotionsschrift unterstützt und begleitet haben.

An erster Stelle möchte ich mich ganz herzlich bei meinem Doktorvater Prof. Dr. Stephan Schreml, Oberarzt der Klinik und Poliklinik für Dermatologie des Universitätsklinikums Regensburg bedanken, sowohl für die exzellente fachliche Betreuung als auch seine warmherzige, unermüdliche wissenschaftliche Unterstützung während der gesamten Bearbeitungsphase meiner Dissertation. Die konstruktive Kritik, die zahlreichen motivierenden Gesprächen werden mir immer als Bereicherung in Erinnerung bleiben.

Des Weiteren möchte ich mich bei Susanne Wallner für die professionelle Einarbeitung in die labortechnischen Färbungsmethoden, die stetig tatkräftige Unterstützung und das große Engagement bedanken. Ihre andauernde Hilfsbereitschaft, Motivation und die fortwährenden Bemühungen haben wesentlich zum Gelingen der Experimente beigetragen.

Mein herzlicher Dank gilt auch Judith Stolwijk, für die viele Zeit, die Verbesserungsvorschläge, die Geduld sich stets kritisch mit meinem Promotionsthema auseinanderzusetzen. Ihre außerordentliche Beteiligung hat maßgeblich zum Erfolg meiner Dissertation beigetragen.

Zu guter Letzt möchte ich meiner Familie und meinem Partner danken, die mich mit grenzlosen Rückhalt und tiefsten Verständnis immer unterstützt haben. Danke, dass ihr an mich geglaubt habt!